Diffusiophoresis, Diffusioosmosis and Microfluidics: Surface-flow-driven phenomena in the presence of flow

Suin Shim*

Department of Mechanical and Aerospace Engineering, Princeton University, Princeton, NJ 08544, USA

E-mail: sshim@princeton.edu

Abstract

Diffusiophoresis is the spontaneous motion of particles under a concentration gradient of solutes. Since the first recognition by Derjaguin and colleagues in 1947 in the form of capillary osmosis, the phenomenon has been broadly investigated theoretically and experimentally. Early studies were mostly theoretical and were interested in surface coating applications due to the directional transport of coating particles. In the past decade, advances in microfluidics enabled controlled demonstrations of diffusiophoresis of micro- and nano-particles. The electrokinetic nature and the typical scales of interest of the phenomenon motivated various experimental studies using simple microfluidic configurations. In this review, I will discuss studies that report diffusiophoresis in microfluidic systems, with the focus on the fundamental aspects of the reported results. In particular, parameters and influences of diffusiophoresis and diffusioosmosis in microfluidic systems and their combinations are highlighted.

Contents

1. Introduction

Diffusiophoresis is the motion of suspended particles (colloids, cells, macromolecules, etc.) that is driven by the bulk concentration gradient of dissolved solute in the liquid phase. The phenomenon was first discovered by Derjaguin and colleagues,[1,2(English translation)] in the form of capillary osmosis. The recognition and the mathematical validation were first made for non-electrolytes, then the analysis was further extended for electrolyte solutions.[3,4(English translation)] In these original studies, the authors discuss the capillary osmosis, particle distribution, and deposition of latex particles on a model surface driven by the non-electrolyte and electrolyte concentration gradients.

The origin of the diffusiophoretic motion is generation of osmotic flow along the particle surface (diffusioosmosis). In non-electrolyte solutions, the direction of this surface flow is determined by the surface-solute interaction.[5–7] When the solute is an electrolyte, the osmotic slip has electrophoretic and chemiphoretic contributions, induced by, respectively, the diffusivity difference(s) among the ions and the osmotic pressure gradient along the surface.[8–10] Near a fixed wall, diffusioosmotic flow is generated along the concentration gradient, and for mobile particles, diffusiophoretic motion is generated.

Early studies were mostly theoretical (with macroscopic experiments)[5–20] and had practical interest in surface coating applications.[21,22] For example, near dissolving steel surfaces in contact with an electrolyte solution, latex particles underwent diffusiophoresis and accumulated at the surface. For particles with a characteristic length (radius) $a = O(1)$ μm, the diffusiophoretic mobility set by the gradient of common salts (e.g. NaCl) is $\sim 10^3$-10^4 times higher than the Stokes-Einstein diffusivity ($D_p = \dfrac{k_B T}{6\pi\mu a}$; k_B and T are, respectively, the Boltzmann constant and absolute temperature). Therefore, increase in the mobility of latex particles was considered advantageous for coating systems. Diffusiophoresis and diffusioosmosis discussed in this paper are good examples of physicochemical hydrodynamical phenomena where the chemical process and flow behaviors occur in the overlapping scales.[23]

When typical diffusiophoresis experiments are set up in microfluidic systems, diffusion of solute, diffusioosmotic flows along the walls, and the particle motion occur simultaneously within the characteristic length and time scales of the system. This can be contrasted to situations where the typical scale of either chemistry or flow behavior is much larger or smaller than the other (e.g. influence of air dissolution on water drop coalescence, influence of oxygen diffusion on the liquid flow speed in PDMS channels, explosion, etc.).

Diffusiophoresis has been of interest to multiple communities since it requires understanding of electrokinetics, species diffusion, fluid mechanics, etc. Diffusiophoresis, as a part of various gradient-driven phenomena, is discussed in the review article by Anderson;[7] as a description of electrokinetics driven by out-of-equilibrium double layers, is reviewed in the article by Dukhin;[24] as a context of osmotically-induced phenomena, is reviewed by Marbach and Bocquet;[25] and multiple origins of concentration gradients for diffusiophoresis are discussed in the review by Velegol et al.[26]

After sixty years of development in theoretical explanations of diffusiophoresis and diffusioosmosis, finally, the use of microfluidics[27] in confirming the enhanced particle motility, was reported in 2008 by Abécassis et al.[28,29] Since then, along with the development of microfluidics, a large number of experimental studies were reported for different channel configurations, and various types of solutes and particles (Table 1). Such experimental studies contributed to the electrokinetics and soft matter communities by directly visualizing the collective particle motion under a concentration gradient of solutes. The current state of understanding is that the main physical concepts and theoretical models of diffusiophoresis can be confirmed by microfluidic experiments. Also, in some studies, diffusiophoresis is unravelled or identified as a main physical mechanism for complex systems, explaining either counterintuitive or previously unknown observations. For the proof of concept experiments, various ways of setting up concentration gradients and corresponding particle motion are listed in the article by Shin.[30]

In this review, I will broadly discuss recent results that illustrate microfluidic experiments

of diffusiophoresis and diffusioosmosis, with particular interests in fundamental aspects of the observed phenomena, rather than focusing on practical applications. In fact, all studies report variations of the original physical picture that Derjaguin et al. provided using theories and experiments.[1–4] Therefore, the goal of this review is to convince the readers that: (i) diffusiophoresis and diffusioosmosis are surface-flow-driven phenomena, (ii) particle motion is relative to the fluid, and so understanding fluid behavior is necessary, (iii) surfaces and concentration gradients are ubiquitous, and (iv) an integrated approach for analyzing diffusiophoresis and diffusioosmosis is required for the next step research.

Typical theoretical models for (electrolyte-driven) diffusiophoresis are obtained within the length scale of the electrical double layer (EDL),[72] and most microfluidic experiments

Table 1: Microfluidic studies peformed for different geometries, particles and solutes.

Systems	Types	Examples of studies	Other references
Geometries	No imposed flows	e.g. Dead-end pores[31–38] Hele-Shaw cell[39,40] Reacting walls[41–43]	Various directions of particle motion and concentration gradients[30]
	Imposed flow	e.g. Co-flow (or flow focusing)[28,29] Solute diffusion through permeable walls[44–49] Reacting walls[50–52] Bridge channel[53–56]	
Solutes	Salt diffusion Ion exchange Gas dissolution	e.g. NaCl, KCl, etc.[...37,57...] e.g. Nafion[41–43,50–52...] e.g. CO_2[40,48,49,59,60]	Non-electrolyte solutions[58]
Particles	Non-reacting colloids	e.g. Polystyrene, Silica, etc.[28,29,31–42,44–48,50–54,61...]	Self-propulsion particles are reviewed in the article by Moran and Posner[71]
	Macromolecules	e.g. Proteins, DNA, etc.[56,62–68]	
	Cells	e.g. Bacteria, blood cells[36,40,43,69,70]	

consider concentration gradients along the channel length of O(100) μm. Also, even though the channel walls contribute as the source of liquid flow by diffusioosmosis, most studies only focused on how the particle distribution is directly related to the imposed solute gradients. Models and experiments match well within the length and time scales that are intended in each study, but such proof of concept research cannot fully explain the role of all system parameters (e.g. varying particle properties, influence of the geometry on fluid flow, etc.) and their combined influences. When complex particles and solutes are considered, as shown in the examples of diffusiophoresis of swimming bacteria[40] and protein-concentration-dependent transport of cell cargo,[68] it is very important to differentiate diffusiophoresis from overlapping multiple transport phenomena. Then the focus of the study is not just about reasonable theoretical prediction of experimental measurements. *What is diffusiophoresis in this system* becomes the first main question. That is why even after great development of theoretical and experimental studies of diffusiophoresis,[7,24–26] we must revisit fundamentals of this surface-flow-driven phenomenon in order to properly apply our understandings to more complex or naturally existing systems (e.g. biological particles, soft particles, complex geometry, or coexistence of multiple physical origins).

In Section 2, theoretical models for diffusiophoresis and diffusioosmosis are introduced with two studies that visualized the influences of the finite double layer thickness and varying surface potentials.[32,35] In Section 3, sources of concentration gradients are discussed. In Section 4, various particles are discussed with a remark that surface-liquid interactions determine the diffusiophoretic behaviors. In Section 5, microfluidic systems and their roles in experimental studies are discussed in terms of solute gradients and fluid flows present in the channels. Finally, in Section 6, potential directions that can be developed by the research communities with academic and practical objectives are suggested. In the step by step review, inclusion of my own work is inevitable, as my recent publications report original findings of complex systems that are not just proof of concept or validation of a simple model. Even though diffusiophoresis and diffusioosmosis can be driven by both non-electrolyte[5,58]

and electrolytes, most recent studies used electrolyte solutions to demonstrate diffusiophoresis of charged particles, so I will discuss electrolyte systems throughout the paper. Also, diffusiophoresis in this article excludes the self-diffusiophoresis of active particles.

2. Diffusiophoresis and diffusioosmosis

When a colloidal particle is suspended in an electrolyte solution, the surface typically obtains a net charge, and a nonzero surface potential forms in the liquid in contact with the surface. Under a concentration gradient of surrounding solutes, the particle migrates along the gradient by diffusiophoresis, relative to the fluid. The main mechanism is that the out-of-equilibrium structure of the electrical double layer (EDL) induces liquid flow along the particle surface, and as a result, mobile particles can move in the direction opposite to the surface flow, due to the viscous stress within the EDL (Figure 1).

2.1. Diffusiophoretic and diffusioosmotic mobility

The physical origin of diffusiophoresis and diffusioosmosis is the same, but in this article I will use both terms to distinguish, respectively, the particle motion and the flow along a stationary surface. In typical microfluidic experiments, as the commonly used channel materials gain nonzero surface charge by contacting electrolyte solutions,[73,74] the solute concentration gradient will generate diffusioosmotic flows along the walls. For a surface with a zeta potential ζ in contact with a z:z electrolyte (e.g. NaCl, NaOH, etc.), a diffusioosmotic flow can be generated along the surface due to the concentration gradient ∇c. The diffusioosmotic velocity is[9,26]

$$u_{do} = -\frac{\epsilon}{\mu}\frac{k_B T}{ze}\left[\beta\zeta - \frac{2k_B T}{ze}\ln\left(1-\tanh^2\frac{ze\zeta}{4k_B T}\right)\right]\nabla\ln c = \Gamma_w \nabla \ln c\ , \tag{1}$$

where ϵ, μ, k_B, T, z and e are, respectively, the electrical permittivity, fluid viscosity, Boltzmann constant, absolute temperature, valence, and the charge on an electron. Γ_w is the diffusioosmotic mobility, and β is the diffusivity difference factor, $\beta = \dfrac{D_+ - D_-}{D_+ + D_-}$, where D_+ and D_- are, respectively, the diffusion constants of the positive and negative ions. The above expression is obtained in the limit of an infinitesimally thin double layer ($\dfrac{\lambda_D}{\ell_c} \to 0$; $\lambda_D = \sqrt{\dfrac{\epsilon k_B T}{2z^2 e^2 c}}$ is the Debye screening length and ℓ_c is the characteristic length scale of the system). For a particle of the zeta potential ζ, the diffusiophoretic mobility Γ_p is then $\Gamma_p = -\Gamma_w$, and the term $\beta\zeta$ indicates the electrophoretic contribution due to the difference in ion diffusivities. From the form of Γ_p, we understand that the local fluid properties (ϵ, μ, ζ), and salt behaviors (β, z, c) are major factors that determine transport of a single particle. Details of the derivation can be found in the article by Prieve et al.,[9] in Section 2.

Prieve and colleagues[9] further analyzed the effect of a finite double layer thickness ($0 < \lambda_D \ll 1$) by considering a spherical particle of radius a. The mobility has the form[9,32,35]

$$\Gamma_p = \frac{\epsilon}{\mu}\left(\frac{k_B T}{ze}\right)^2 \left(\frac{u_0(\zeta)}{1 - \frac{\lambda_D}{a}\frac{u_1(\zeta,\alpha^*)}{u_0(\zeta)}}\right), \tag{2}$$

where u_0 is the leading-order term $u_0(\zeta) = \beta\zeta - \frac{2k_B T}{ze}\ln\left(1 - \tanh^2\frac{ze\zeta}{4k_B T}\right)$, and $\frac{u_1}{u_0}$ is the $O\left(\frac{\lambda_D}{a}\right)$ correction, with α^* defined as $\alpha^* = \frac{\epsilon(k_B T/ze)^2}{\mu D_a}$. D_a is the characteristic (ambipolar) diffusivity of the ions, and for a z:z electrolyte, $D_a = \dfrac{2D_+ D_-}{D_+ + D_-}$.

Unless the system is set up to have binary salts only, most of the naturally existing systems have multiple ions present. The diffusioosmotic velocity along a surface driven by a concentration gradient of multiple electrolytes with arbitrary valences (z_i) can be obtained by considering coupled ion fluxes[75]

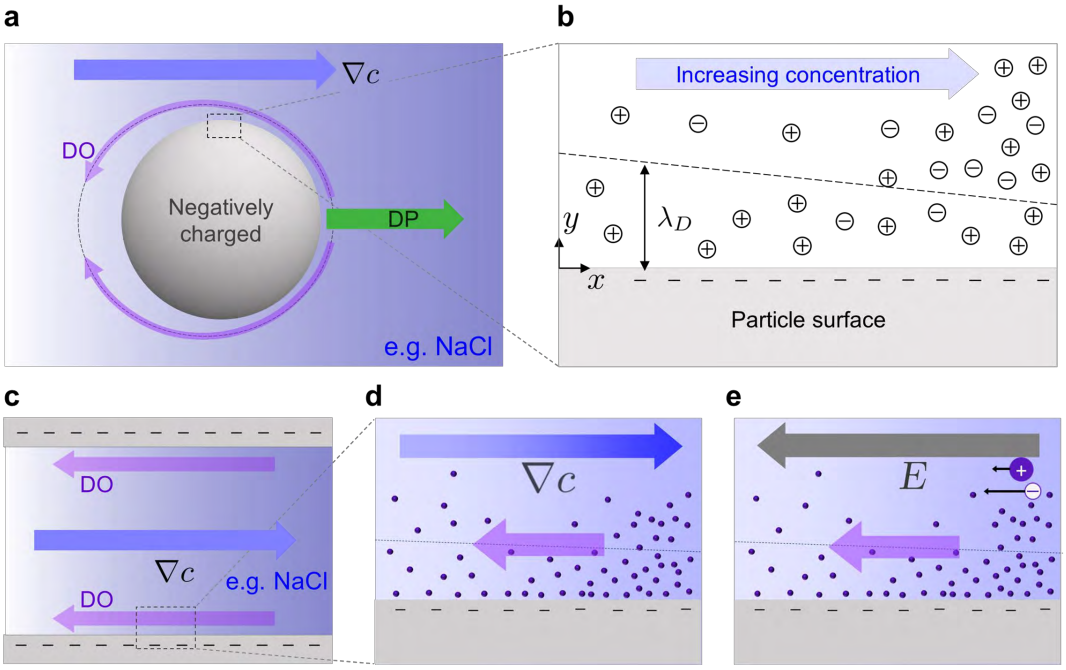

Figure 1: Diffusiophoresis of a particle and diffusioosmotic flow along a surface. (a) Schematic of a concentration gradient of NaCl and a negatively charged particle. Diffusioosmotic flow (DO) is generated along the particle surface, and the resulting diffusiophoretic motion (DP) is toward high concentration. (b) Schematic of the surface region of the particle, illustrating the non-uniform double layer due to an ion concentration gradient. (c) Schematic of diffusioosmotic flow generated along two parallel walls. (d,e) Schematics of (d) chemiosmosis and (e) electroosmosis, respectively. The dots represent counterions, and the case of negative β (e.g. for NaCl) is described. The same surface flow is generated along the particle surface in shown in (a), making the particle move in the opposite direction. See supporting video S1 for animated explanations.

$$u_{do} = -\frac{\epsilon}{\mu}\left(\frac{k_B T}{e}\right)^2 \left[\frac{\sum_i D_i z_i \nabla c_i}{\sum_i D_i z_i^2 c_i}\Psi_D - \frac{1}{2}\sum_i \left(\nabla c_i \int_0^{\Psi_D} \frac{\left\{\int_0^{\Psi_0} g_i(\Psi')\left[\sum_j c_j g_j(\Psi')\right]^{-\frac{1}{2}} d\Psi'\right\}}{\left[\sum_j c_j g_j(\Psi_0)\right]^{\frac{1}{2}}} d\Psi_0\right)\right], \tag{3}$$

where Ψ_D is the nondimensional surface potential $\Psi_D = \dfrac{\zeta e}{k_B T}$ and $g_i(\Psi_0) = \exp(-z_i\Psi_0) - 1$. The properties with the subscript i are that of the i^{th} species.

For small surface potential, $\Psi_D \ll 1$, the flow velocity reduces to the form of[76]

$$u_{do} = -\frac{\epsilon}{\mu}\left(\frac{k_B T}{e}\right)\frac{\sum_i D_i z_i \nabla c_i}{\sum_i D_i z_i^2 c_i}\zeta - \frac{\epsilon}{8\mu}\frac{\sum_i z_i^2 \nabla c_i}{\sum_i z_i^2 c_i}\zeta^2 \ . \tag{4}$$

For a mobile particle with the same surface and electrokinetic properties, the diffusiophoretic velocity $u_{dp} = -u_{do}$.

2.2. Surface interaction with electrolytes

As we can deduce from the form of the flow velocity, the surface potential plays an important role on diffusioosmosis. The surface zeta potential, which is a theoretical parameter, is defined as a potential drop across the electrical double layer (between the shear plane and the bulk; Figure 2). This value is not an absolute material property, and most colloidal particles and surfaces that we use in microfluidic experiments have varying zeta potentials depending on the interaction with the contacting liquid.[73,74,77–79] For example, polystyrene (PS) microspheres were commonly used in recent studies, and it has been studied and measured that the surface potential varies with pH and electrolyte concentrations of the reference solutions.[74,77]

Theoretically, as the zeta potential is a characterization of the double layer, there are two

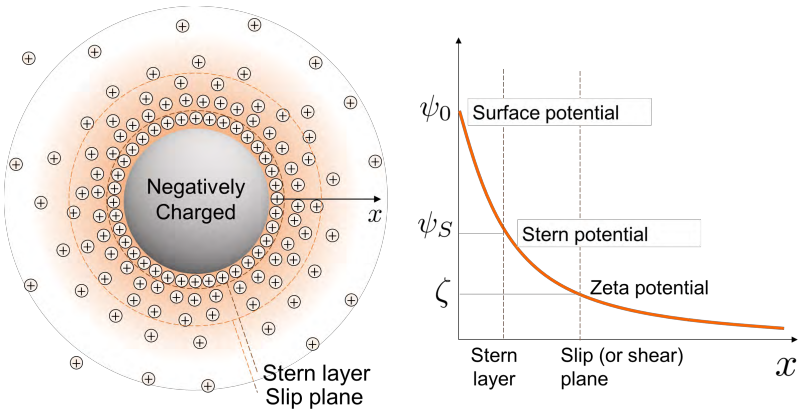

Figure 2: Schematic of a negatively charged particle and counterions. Different electrical potentials in the diffuse double layer are indicated.

different limits, where ζ is constant or the surface charge density q is constant. Polymeric surfaces are usually in between these two limits, and can be described with a charge-regulation model.[80] A constant charge density condition requires q to be constant and is related to the potential drop across the double layer. Considering the Boltzmann distribution of ions in the double layer, we obtain

$$\sum_i c_i(\exp(-z_i\Psi_D) - 1) = \text{constant} \tag{5}$$

for multiple electrolytes.[38,75] For a symmetric (z:z) electrolyte, the Gouy-Chapman solution for the boundary layer yields[35]

$$\frac{\lambda_D^{\text{ref}}}{\lambda_D}\sinh\left(\frac{\zeta}{2}\right) = \sinh\left(\frac{\zeta_{\text{ref}}}{2}\right) \ , \tag{6}$$

where λ_D^{ref} and ζ_{ref} are, respectively, the Debye length and zeta potential at a reference salt concentration c_{ref}.

In systems without significant variation of pH or electrolyte concentrations, it is reasonable to assume a constant surface potential, and so a constant diffusiophoretic mobility. The Debye length λ_D is typically much smaller compared to the particle size ($O(1)$ μm) or the channel wall length ($O(10)$-$O(1000)$ μm). For example, in a 10 mM NaCl solution, the double layer thickness is $\lambda_D = \sqrt{\dfrac{\epsilon k_B T}{2z^2e^2c}} \approx 3$ nm. Therefore, in diffusiophoresis studies using micron-sized particles and 1:1 electrolyte, the mobility is often estimated using equation (1).

Two recent experimental studies using a dead-end pore geometry directly confirmed the effect of finite double layer thickness (equation (2)) by varying the particle size[32] and varying the electrolyte concentrations in the system.[35] In the dead-end pore systems, diffusiophoretic motion of particles along a one-dimensional gradient of salt concentration can be characterized by analyzing the particle distribution inside the pores.[31–38] Usually, the concentration gradients are set up so that the particles move toward the dead-end of the pores, and the position of maximum particle concentration (peak) along the pore is compared with the

theory. More details of dead-end pore geometry will be included in Section 5.

In the first set of experiments,[32] polystyrene particles with different sizes showed different distributions in the dead-end pores. Along the same concentration gradient of NaCl set by the initial pore concentration $c_i = 2$ mM and the boundary concentration $c_o = 0.02$ mM, PS particles with a diameter $d = 0.06$ μm travelled the least in the pores, whereas particles with $d \approx 1$ μm entrained farthest into the pores. Such trend for the peak location is consistent with the model prediction including the finite double layer thickness ($\lambda_D/a \neq 0$) effect with a constant ζ. If the diffusiophoretic mobility is estimated using equation (1), such variations in the particle distribution cannot be explained. The authors also used the Stokes-Einstein diffusivity of a particle $D_p = \frac{k_B T}{6\pi\mu a}$ to qualitatively explain the larger dispersion of smaller particles in the pores.

In the study by Gupta et al.,[35] four different conditions for diffusiophoretic mobility calculation were reported and compared with the dead-end pore experiments. The diffusiophoretic mobility model for a spherical particle (equation (2)) can be analyzed for different combinations of zero ($\lambda_D/a \to 0$) versus finite double layer thickness ($\lambda_D/a > 0$), and constant potential (CP) versus constant charge density (CC) conditions. The authors wrote $\lambda_D/a = 0$ versus $\lambda_D/a \neq 0$ for two different conditions for the effects of double layer thickness. When a finite double layer is considered ($\lambda_D/a \neq 0$), CP condition yields monotonically increasing Γ_p for increasing ion concentration c, and the CC condition makes Γ_p increase to a peak value around $c = O(1)$ mM, then decrease. For $\lambda_D/a = 0$, the CP condition gives a constant Γ_p, and the CC condition makes Γ_p increase dramatically for small c, because the surface potential increases to meet the constant charge density (following $\lambda_D^{-1} \sinh(\zeta/2) = \text{constant}$).[35] This overestimation of the surface potential for small c in the CC limit (with the $\lambda_D/a = 0$ condition) even suggested an unphysical diffusiophoretic mobility, which is larger than the solute diffusivity. According to the comparison with the dead-end pore experiments, constant charge density (CC) condition including the finite double layer effect ($\lambda_D/a \neq 0$) well predicted the behavior of polystyrene particles.

2.3. Remarks on diffusiophoretic velocity of particles

The studies confirming the influence of finite double layer thickness and varying zeta potential leave a few important messages about analyses or applications of relevant systems. When discussing boundary or limiting conditions based on the theoretical model (e.g., zero solute concentration, systems without walls, sharp initial concentration gradient, etc.), careful consideration of the underlying physics is required. For example, Gupta et al.[35] introduces calculations for diffusiophoretic velocities generated by a one-dimensional diffusion of a solute, which initially has a Gaussian distribution. They compare two solute (NaCl) profiles in the form of $c(X,\tau) = \frac{c_0}{\sqrt{1+4\tau}} \exp\left(-\frac{X^2}{1+4\tau}\right) + c_b$, by setting (i) $c_b = 0$ and (ii) $c_b = 10^{-7}$ M. In this model problem, the solutes freely diffuse in X, and the diffusiophoretic velocity generated by the solute concentration gradients can be calculated. Typically, when formulating a model study, water without any solute of interest is often considered as a zero ion concentration medium.

Using the values $c_0 = 11.8$ mM and $c_{\text{ref}} = 5$ mM, the authors report that if the background concentration $c_b = 0$, the zero double layer approximation (equation (1)) gives increasing diffusiophoretic velocity (both CC and CP) in the regions that the ions have not yet diffused, which is unphysical. In this case, only by looking at the monotonically increasing velocity for large X, can one suggest that such spreading of solute induces ballistic motion[81] of particles for large X. However, the definition of λ_D tells that a small ion concentration yields large λ_D, which thus suggests that the finite double layer effect must be included. By doing so, the diffusiophoretic velocity is calculated to be zero in the regions of no solute. When the background ion concentration c_b is set to be $c_b = 10^{-7}$ M, the diffusiophoretic velocity is $u_{dp}(X,\tau) = \Gamma_p \frac{\partial \ln c}{\partial X} = -2\alpha \left(\frac{u_0}{1-\frac{\lambda_D u_1}{a u_0}}\right)\left(\frac{c-c_b}{c}\right)\frac{X}{1+4\tau}$, and the small $\frac{c-c_b}{c}$ for large X gives increasing then dicreasing velocity profiles for increasing $|X|$ for all four surface characterizations.

If we develop theoretical analyses for diffusiophoresis only by considering a constant

mobility (equation (1); CP and $\lambda_D = 0$), the logarithmic dependence on solute concentration may predict a huge diffusiophoretic velocity for situations of $c \to 0$. However, such behavior is unphysical and unlikely to be achieved in the experimental or natural situations. For $c \to 0$, the length scale of the double layer becomes comparable to a typical microsphere, and for large c, charge screening near a surface can reduce the surface potential significantly,[74] which decreases the diffusiophoretic mobility.

Consideration of the particle size and zeta potential dependence on the diffusiophoretic mobility motivated development of the measurement and sorting applications.[16,32,56] Diffusiophoretic and diffusioosmotic determination of a surface potential is similar to the electrophoretic methods, but since the solute concentration is not constant, one need to admit the limitation that the estimated surface potential is a representative value of a range that corresponds to the range of solute concentration used in the measurement system.

3. Solute concentration gradient

Next, I will briefly mention several sources of concentration gradients in microfluidic experiments. More details of the origin of concentration gradients can be found in the review by Velegol et al.[26]

3.1. Diffusion of salt

Most experimental studies utilized simple binary salts (NaCl, KCl, LiCl, etc.), and for biological particles, concentration of either buffer or test salts were varied. The concentration gradients of acid and base can be set up to create both pH and ion concentration gradients (Figure 3(a)). Such system requires additional analyses of the influence of pH on diffusiophoresis (or surface properties).[46,82,83] It was also demonstrated that ionic surfactants[36,39,47,84,85] (Figure 3(b)) can drive diffusiophoretic transport of charged particles, and thus capable of contributing to detergency efficiency.[84] Multi-ion systems and diffusiophoresis

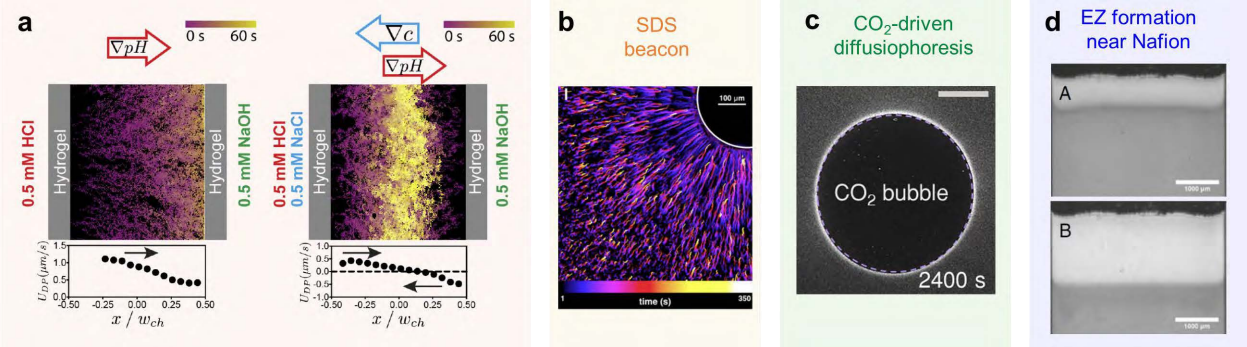

Figure 3: (a) Diffusiophoretic focusing induced by combined concentration gradients of NaCl, HCl, and NaOH. Reproduced with permission from ref.[46] Copyright 2016 American Physical Society. (b) Trajectories of polystyrene particles near the source of sodium dodecyl sulfate (SDS). Reproduced with permission from ref.[39] Copyright 2016 National Academy of Sciences. (c) CO_2-driven diffusiophoresis of amine-modified polystyrene. Reproduced with permission from ref.[40] Copyright 2021 Royal Society of Chemistry. (d) Exclusion zone (EZ) formation near the ion exchange membrane (Nafion). Reproduced with permission from ref.[41] Copyright 2014 National Academy of Sciences.

driven by asymmetric salts were also investigated.[37,38,46,50–52,76]

3.2. Dissolution of gas

Ion concentration gradients can be generated by dissolution of gas. CO_2-driven diffusiophoresis of charged particles are reported in various configurations.[40,48,49,59,60] CO_2 dissolution and dissociation creates H^+ and HCO_3^- ions and induce electrophoresis-dominated diffusiophoretic motion of charged particles. Dissolution of CO_2 in water can be achieved at the gas-liquid interface[40] (Figure 3(c)), or through gas-permeable membrane.[40,48,49,60] It has been demonstrated that bacterial cells,[40] fluorescent protein,[59] and oil nanoemulsion-particle pair[60] can migrate by CO_2-driven diffusiophoresis.

3.3. Surface reaction and other sources

Early studies reported surface coating of latex particles induced by the dissolution of stainless steel[21,22] Florea et al.,[41] first explained the formation of an exclusion zone near an ion exchange membrane, Nafion, by diffusiophoresis argument (Figure 3(d)). Since then, Nafion appeared in several experimental studies[42,50–52] for diffusiophoretic particle separation. Der-

mott et al.[86] presented diffusioosmotic flow generated by $CaCO_3$ and $BaSO_4$ micropumps.

As seen in the original study by Ramm et al.,[68] a density gradient in proteins can cause migration of other macromolecules. A concentration gradient of solute can be also set up by other phoretic effects (e.g. thermophoresis), and then induce diffusiophoresis or diffusioosmosis. Such configuration is discussed in the article by Fukuyama and Maeda.[87] Note that concentration gradient of solutes can be created by both addition and depletion of solutes.

4. Particles used in experimental studies

4.1. Microspheres

Theoretically, colloids with a nonzero surface potential under concentration gradients of electrolytes can obtain a diffusiophoretic mobility. Polystyrene (PS) and silica microspheres were popular and appeared in most experimental studies that aimed for both fundamental understanding and applications[28,29,32,34,35,37–42,46–48,50–52,59,61,84,86,88–90] (Figure 4). Polystyrene microspheres have a well-defined surface potential (it is still a function of surface charge density) and sizes. Also, depending on the surface modification (e.g. carboxylate-, sulfate-, amine-modified polystyrene), a range of surface properties can be obtained. In recent diffusiophoresis studies, fluorescent microparticles were used to visualize relative or absolute concentrations of particles. These particles are highly resistant to photobleaching, and thus an appropriate imaging calibration and controlled total particle concentration yields a linear relation between the number of particles and the measured intensity.[37,38]

Typical analyses for diffusiophoresis of particles are conducted for their collective behaviors and change in the distribution. For a system with a binary salt and dilute particle suspension, a model for calculating solute (c) and particle concentrations (n) is

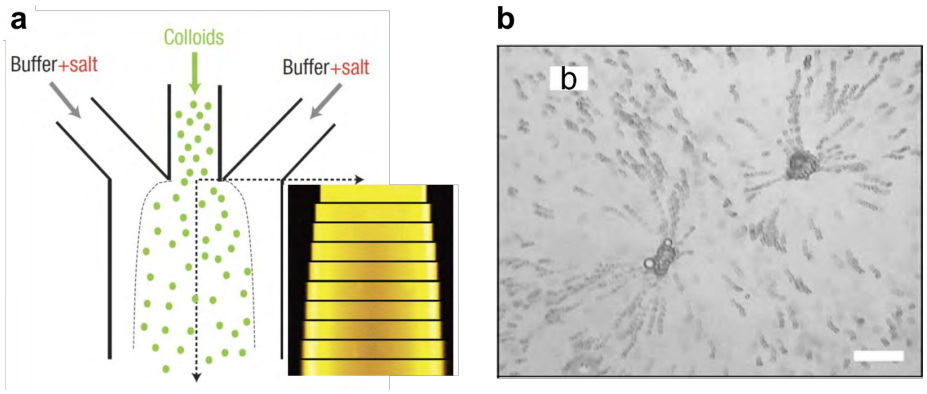

Figure 4: (a) Diffusiophroesis of silica particles in a flow-focusing channel. Adapted with permission from ref.[28] Copyright 2008 Nature Publishing Group. (b) Visualization of diffusioosmotically transported sulfate-modified polystyrene (s-PS) particles near two interacting $CaCO_3$ micropumps. Reproduced with permission from ref.[86] Copyright 2012 American Chemical Society.

$$\frac{\partial c}{\partial t} + \nabla \cdot (\mathbf{u}_f c) = D_a \nabla^2 c \tag{7}$$

$$\frac{\partial n}{\partial t} + \nabla \cdot (\mathbf{u}_p n) = D_p \nabla^2 n. \tag{8}$$

Here, $\mathbf{u}_f$ is the fluid velocity, and the particle velocity is $\mathbf{u}_p = \mathbf{u}_f + \mathbf{u}_{dp}$. Particle distribution is obtained by solving the advection-diffusion equation where the advective velocity is a contribution from both the local flow and the diffusiophoretic velocities. When experiments are designed to maintain a dilute particle limit (to avoid particle-particle interactions), the (rescaled) fluorescent intensity obtained from image analyses can be directly compared with the calculated n. Properties of such commercial microspheres are well characterized in most experimental studies, and thus a few details are discussed in the later sections.

4.2. Proteins and other macromolecules

Advances in microfluidics largely contributed to manipulating and visualizing transport of biological materials. As biological macromolecules such as protein, DNA, vesicles, etc. have typical length scales between $O(10^{-2})$-$O(10^{1})$ μm and have a net surface charge in aqueous solutions, various electrophoretic techniques are used for separation.[91–93] For diffusiophoresis,

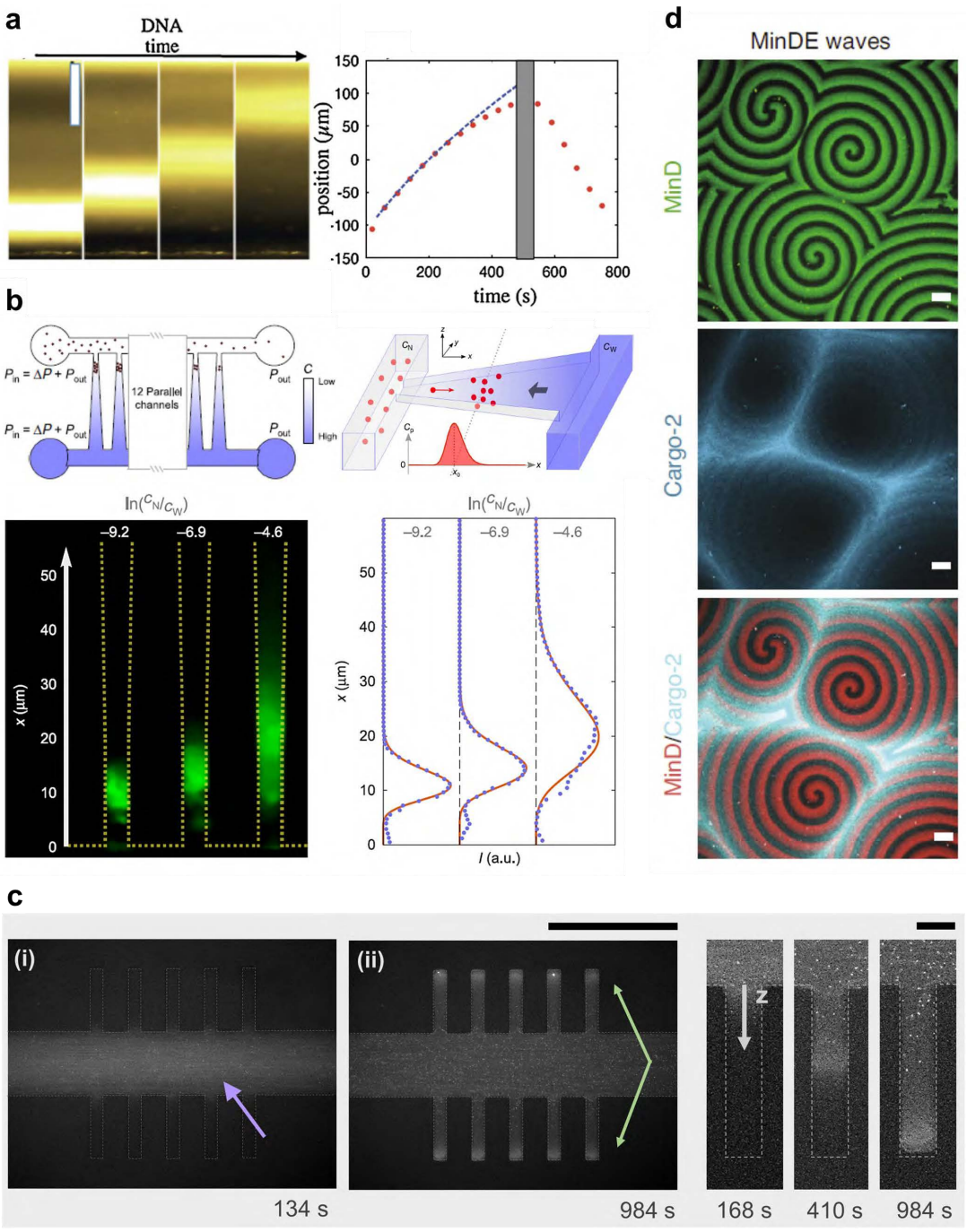

Figure 5: Diffusiophoresis of (a) DNA, (b) exosomes, (c) fluorescent protein mKO (monomeric Kusabira Orange), and (d) cellular cargo, driven by MinDE travelling surface waves, which established long-range concentration gradients. The figures are reproduced with permission from (a) ref,[62] Copyright 2010 American Physical Society, (b) ref,[56] Copyright 2020 Nature Portfolio, (c) ref,[59] Copyright 2020 National Academy of Sciences, and (d) ref.[68] Copyright 2021 Nature Research.

theoretical models for predicting the mobility are derived for a single particle, but the models are not fully refined for particles with complex configurations (shape, non-uniform surface properties, etc.). Diffusiophoresis and diffusioosmosis are relative motion of a surface and adjacent liquid in the low Reynolds number limit ($\mathrm{Re} \ll 1$), and thus geometrical asymmetry affects the velocity measurements.

A microfluidic approach for diffusiophoresis of macromolecules is demonstrated by Palacci et al. for DNA focusing,[62,63] and later more groups visualized and studied diffusiophoresis of lipid vesicles, DNA, proteins and other macromolecules.[32,56,59,66–69,94–98] In the studies by Palacci et al.,[62,63] under a concentration gradient of LiCl set up across the flow, colloidal particles and λ-DNA showed transient diffusiophoretic focusing. The measurements and calculations for the peak propagation indicated that fluorescent-tagged λ-DNA behaves similarly to the polystyrene particles (carboxylate-modified PS; $d = 200$ nm). The diffusiophoretic mobility was the fitting parameter for the study, and their diffusiophoretic focusing experiments provided a reasonable measure of Γ_p by data fitting (Figure 5(a)).

Physicochemical hydrodynamical charateristics are not fully known for various biomaterials. Thus it is crucial that a systematic experimental design is developed to distinguish overlapping physical phenomena, and that a reasonable quantification for various system parameters is achieved. Similar to the method that Palacci et al.[62,63] used to fit the peak propagation using a representative Γ_p, it is reported by Rasmussen et al.[56] that the exosomes (nanometer-sized extracellular vesicles) can be diffusiophoretically sorted by their size and surface potentials (Figure 5(b)) in a microfluidic channel. The authors designed a H-shaped microfluidic channel with a linearly varying width of the bridges (or pores), and were able to trap the vesicles in the pores along different concentration gradients of solutes. Diffusioosmotically driven flow velocity (induced along the pore walls) and particle diffusiophoresis were balanced and it ensured stable focusing of the vesicles. By setting multiple ranges of solute gradients and analyzing the one-dimensional distribution of trapped vesicles, reliable values for the size and representative zeta potential were obtained.

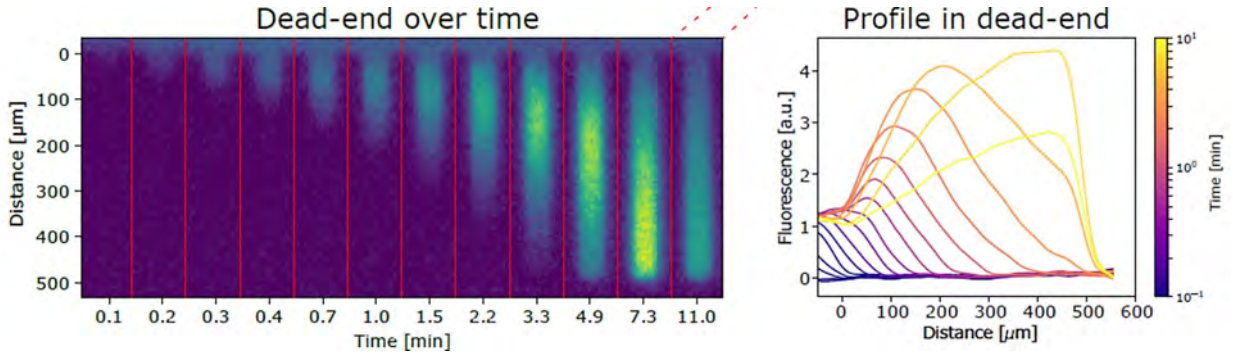

Figure 6: Diffusiophoresis of protein in the dead-end pore geometry and detection of fluorescent intensity. Images reproduced from ref[94] with permission.

Proteins experience a change in surface potential depending on the pH of surrounding medium. For this reason, isoelectric focusing (or electrofocusing) is used as a means for extracting proteins with an imposed electric field.[91,92] Different proteins have different isoelectric points (pI) depending on their chemical and physical structures, so a pH gradient combined with electrophoresis can separate proteins with different charges. This means that a similar technique can be applied with diffusiophoresis by replacing the electric field with a solute concentration gradient. This specific setting is not yet reported, but there have been studies about diffusiophoresis of protein in the context of ternary diffusion system. In the studies led by Annunziata et al.,[97,99] diffusiophoresis of lysozyme using salt gradients (NaCl, KCl, $MgCl_2$) was reported. The authors provided an estimation of the zeta potential and mentioned potential microfluidic application using $MgCl_2$. One-dimensional diffusiophoresis of bovine serum albumin (BSA), β-lactoglobulin, myoglobin, and lysozyme under gradient of LiCl, KCl, and KIO_2 are also demonstrated by Peter et al.[94] using a dead-end pore geometry (Figure 6).

Protein diffusiophoresis has also been observed in unexpected situations. Shim and Stone[59] reported a flow-driven diffusiophoretic focusing driven by the leakage of CO_2 through PDMS walls. In a microfluidic channel, the onset of flow created a nonzero pressure gradient across the PDMS walls and induced leakage of CO_2, which then generated an ion concentration gradient in the aqueous phase. Therefore, polystyrene particles showed charge-

dependent accumulation in the flow. When fluorescent-protein-tagged bacterial cells flowed in the channel, the fluorescent proteins (mKO; monomeric Kusabira Orange) that were in the liquid phase (lysed from cells) behaved like positively charged particles, and were separated from the cell suspension (Figure 5(c)). Estimation of the isoelectric point suggested that the mKO molecules are positively charged in the experimental condition (pH = 6-7), and thus the observation is consistent with the diffusiophoresis idea.

Diffusiophoretic migration of biological particles can be detected not only in the laboratory-designed experiments, but also in natural systems. Theoretically it has been suggested that, inside a cell, a gradient of small molecules that are related to metabolism can drive motion of larger particles.[100] Recently, it has been experimentally demonstrated by Ramm et al.,[68] that a density (concentration) gradient in MinD and MinE proteins can induce transport of cargo on membranes. They report both in vitro and in vivo demonstrations of cargo accumulation in the regions of low protein concentration, with a step by step validation that the main mechanism is diffusiophoretic transport (Figure 5(d)). The study is meaningful in the sense that it provides a new insight and potential path for unravelling intracellular transport of complex biomaterials.

4.3. Cells

Diffusiophoretic transport of living cells is of interest in several studies as the surface of cells have a nonzero charge. Concentration gradient being the origin of the phenomenon is analogous to chemotaxis. For this reason, the terms diffusiophoresis and chemotaxis can sometimes be confused. However, treating diffusiophoresis and chemotaxis as the same phenomenon may not be helpful for the research of diffusiophoresis of chemotactic bacteria, because chemotaxis is an *active* response of the cells to the local chemistry.

Diffusiophoresis of living cells are visualized in several studies, by utilizing a dead-end pore geometry,[36,69] Hele-Shaw cell,[40] channel flow configuration with and without grooves.[59] For example, Doan et al.[36] demonstrated bacterial diffusiophoresis under one-dimensional

concentration gradients of NaCl and surfactants, reporting enhanced diffusiophoresis in the presence of ionic surfactants ($\leq$ 1 mM). The authors interpret the consistent results by presenting an increase in zeta potential measurements in the presence of surfactant. Hartman et al.[69] reported diffusiophoretic transport of blood cells along the concentration gradient of solutes (Sucrose, NaCl, etc.). In the study by Shim and Stone[59] on the CO_2-leakage-driven diffusiophoresis, separation of *V. cholerae* cells and the fluorescent protein (mKO) is reported (Figure 5(c)).

As stated above, some motile bacterial cells swim in the liquid phase by sensing the local concentration of relevant solutes,[101–103] and this active response of bacteria to the chemical concentration gradient is chemotaxis. From early times of diffusiophoresis research[6,7] it had been speculated that salt-driven phoretic behavior of bacteria could be related to diffusiophoresis. Due to the overlapping idea that a concentration gradient of local electrolytes

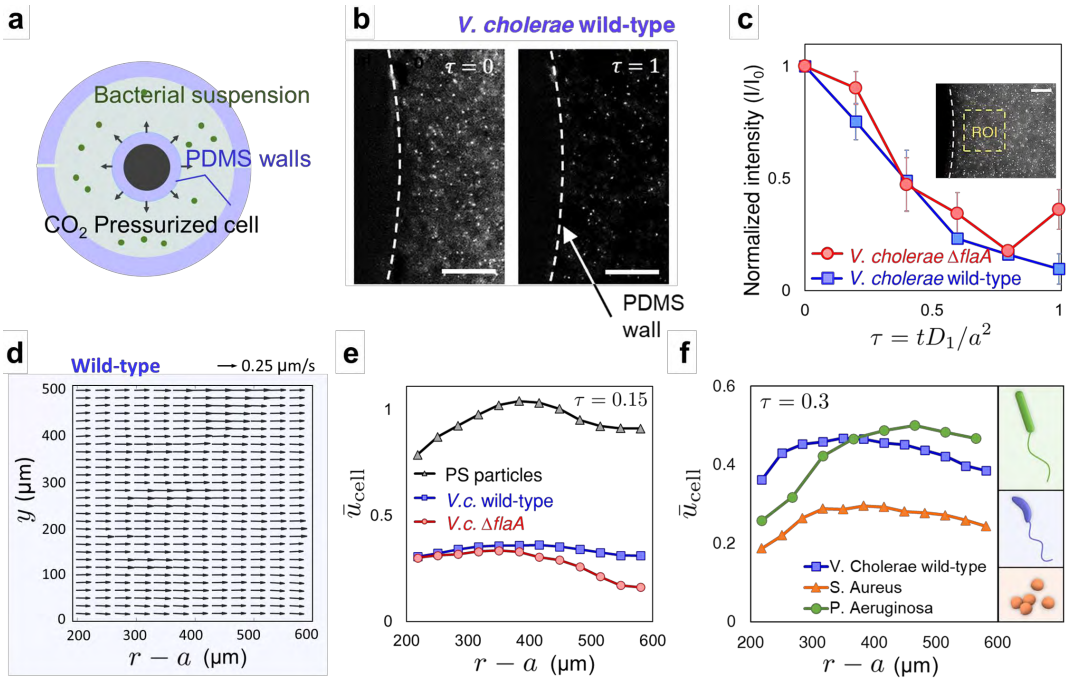

Figure 7: CO_2-driven diffusiophoresis of bacterial cells in a circular Hele-Shaw geometry. (a) Schematic of the system. (b,c) Fluorescent images and the intensity plot visualizing decrease in cell density near the CO_2 source. (d-f) Particle image velocimetry showing different diffusiophoretic velocities of bacterial strains. Images reproduced with permission from ref.[40] Copyright 2021 Royal Society of Chemistry.

causes the motion, experiments need to be carefully designed to ensure that the observed motion is diffusiophoresis, not chemotaxis.

Shim et al.[40] reported diffusiophoresis of bacteria driven by dissolution of CO_2 in a circular Hele-Shaw geometry. CO_2 is not a chemoattractant or repellent (though it may affect the performance of flagellar motors by perturbing the system pH), and its dissolution in water can set up high diffusion potential by the large difference in ion diffusivities ($D_{H^+} = 9.3\times10^{-9}$ m^2s^{-1} and $D_{HCO_3^-} = 1.2 \times 10^{-9}$ m^2s^{-1}). Therefore, an effective demonstration of bacterial diffusiophoresis is possible near the CO_2 source that has either a moving or a fixed boundary (Figure 7).

Bacterial cells (*V. cholerae*, *S. aureus*, and *P. aeruginosa*) have a negative surface charge in the dilute buffer solution (M9 minimal salt), and the cells undergo diffusiophoresis away from the fixed CO_2 source (Figure 7(a-c)). Particle image velocimetry (PIV; Figure 7(d-f)) first indicates that both the wild-type (WT) and the non-motile mutant (Δ*flaA*) of *V. cholerae* show radially-outward motion of the cells away from the CO_2 source. This directly confirms that the measured velocity is that of diffusiophoresis, because if it were chemotaxis, the non-motile bacteria need to be stationary. The small difference in the velocity between the WT and Δ*flaA* mutant may arise due to their motility difference.

When different types of bacteria (*V. cholerae* (WT), *S. aureus*, and *P. aeruginosa*) are compared, *S. Aureus* showed the slowest diffusiophoresis under the same ion concentration gradient. The reported zeta potential values for *P. Aeruginosa* and *S. Aureus* are $\zeta \approx -30$ mV, and the velocity difference cannot be fully explained by the surface potential argument of diffusiophoresis. The authors state that for *S. aureus*, surface adhesive proteins make the cells easily form clusters, which may contribute to the change in the diffusiophoretic velocity. The difference in diffusiophoretic velocities among different species may also arise from different aspect ratios of the cell bodies. Therefore, the study validates that bacterial cells do undergo diffusiophoresis due to the charged nature of the cell surface, but their diffusiophoretic velocities are not completely described with the zeta potential.

In such situations where physical (e.g. shape, rigidity, etc.) properties and biological (e.g. secretion of chemicals) behaviors of the particles affect diffusiophoretic mobility, they can also influence the electrophoretic mobility under an imposed electric field; and thus can bias the zeta potential value obtained by the electrophoretic zeta potentiometry. Note that commercial zetasizers require bulk liquid properties for zeta potential measurements. Then using only the zeta potentiometry data to explain the diffusiophoresis behavior is insufficient, and it may lead to a conclusion that neglects important structural and biological consequences of the system.

4.4. Remarks on particles

Synthetic colloids with well-controlled surface properties are excellent tools for studying diffusiophoresis. On the other hand, by using diffusiophoresis, surface characteristics of such materials can be estimated as well. Zeta potential of particles is conveniently used as the main surface property when measuring or estimating the diffusiophoretic mobility. As mentioned earlier, zeta potential is not a fixed particle material propery. It is a theoretical quantity that is defined in the liquid in contact with the particle surface, and thus the value changes

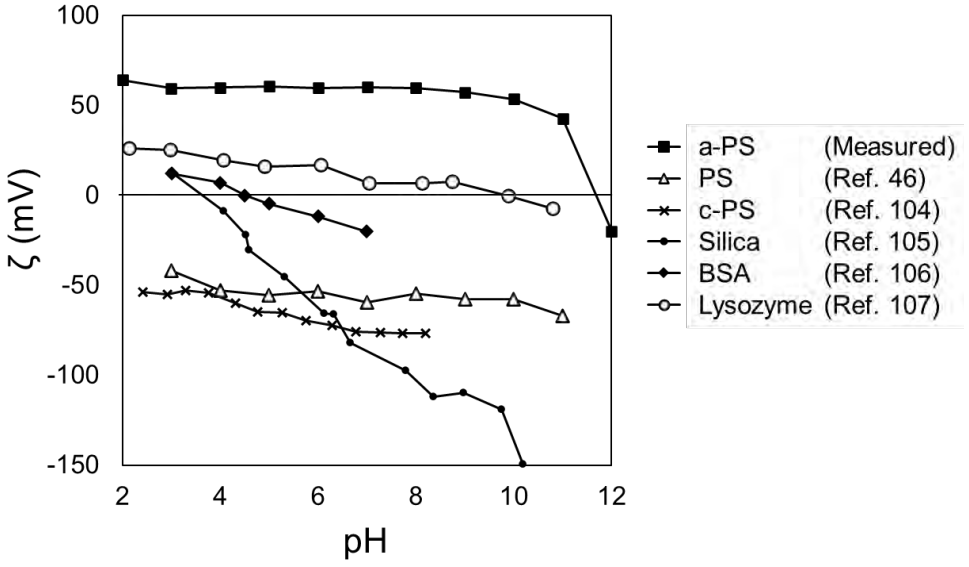

Figure 8: Zeta potential of various particles plotted versus pH. The data are obtained from various references for PS,[46] c-PS,[104] Silica,[105] BSA,[106] and Lysozyme,[107] respectively.

if the liquid condition changes (e.g. pH). In Figure 8, zeta potential of several kinds of particles are plotted versus pH.[46,104–107] Commercial polystyrene particles with and without functional groups (PS, amine-modified PS; a-PS, and carboxylate-modified PS; c-PS) have approximately constant potential over a wide range of pH (except for a sharp decrease for a-PS near pH = 11), and silica particles show negative surface potential for pH>4. Proteins (BSA and lysozyme) show varying surface potentials and have isoelectric points. Details on the zeta potential of various materials commonly used in microfluidic experiments can be found in the review article by Kirby and Hasselbrink Jr.[73,74]

Experimental studies that validate theoretical models (e.g. equations (1-4)) provide a good basis for extending the investigations for diffusiophoresis of biological particles. For such complicated systems, experimental design and analyses must be done carefully, to distinguish diffusiophoresis from other coexisting biophysical phenomena. When it comes to studying diffusiophoresis of intracellular materials, accounting for various scales of multiple transport phenomena can be helpful in the designs for independent (in vitro) experiments.

Bacterial diffusiophoresis has been of interest among researchers due to its salt-taxis nature. It has been confirmed that both motile and immotile bacteria can move along a concentration gradient of CO_2,[40] salt, and surfactant.[36] The next steps of the research can focus on detailed investigation of solute-cell interaction. For example, if the solute is a chemoattractant, its electrokinetic contribution to the diffusiophoretic mobility, chemical influence on the chemotactic motility, and the differences in individual and collective motion need to be analyzed. In the study by Shim et al.[40] the measured diffusiophoretic velocities were lower than the random swimming velocities of motile bacteria, suggesting that separation of scales may be helpful for distinguishing the two phenomena. Another example for the solute-cell interaction can be changes in local fluid properties due to the secretion of cell material on the surface (e.g. biosurfactants), produced by regular metabolism or cell lysis procedure. If the electrical permittivity ϵ and the liquid viscosity μ in the small region near the cell surface are different from the bulk experimental medium, it is likely that both ap-

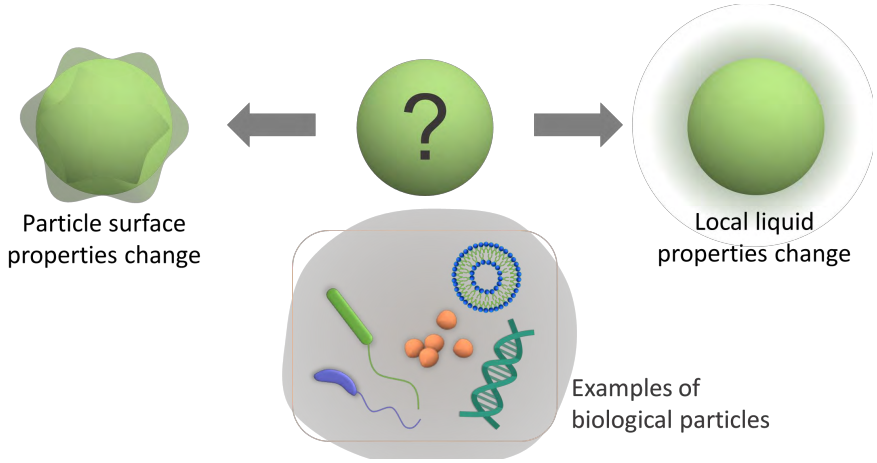

Figure 9: Schematics describing changes in the particle conformation and the changes in local liquid properties induced by solute-particle interactions, which can be present in biological particles (e.g. cells, vesicles, DNA, etc.).

parent electrophoretic and diffusiophoretic velocities deviate from the values estimated using the bulk properties. Changes in the cell conformation induced by biological processes and its influence on diffusiophoresis can be also a theme for the next step research (Figure 9).

Diffusiophoresis of reacting particles[71,108,109] and liquid drops[110,111] are not included in the review. Studies of both passive diffusiophoresis and self-diffusiophoresis are of active interest, and further development is anticipated in terms of theoretical and experimental aspects, or in combination.

5. Microfluidic systems

In this section, the role of microfluidic systems in experimental studies of diffusiophoresis and diffusioosmosis is discussed. The primary role of microfluidic experiments is to set up a desired concentration gradient of solutes and to achieve corresponding particle motion. However, due to the charged surfaces of the system (e.g. PDMS channel walls) and the existence of bulk liquid flow, often the observed particle motion is not just a result of diffusiophoresis. Therefore, I will point out such influences of various system parameters when discussing selected flow systems. One common feature is that the typical length scale of the

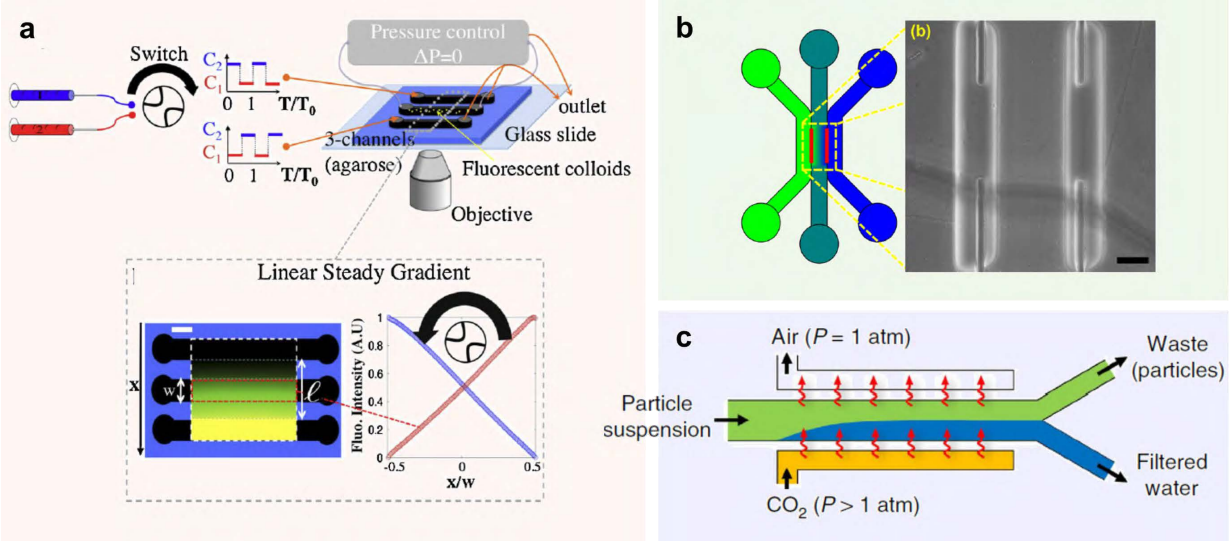

Figure 10: Diffusiophoresis experiments in three-channel systems. (a) Switching concentration gradient is obtained in the agarose gel channel. Reproduced with permission from ref.[62] Copyright 2010 American Physical Society. (b) A semipermeable wall (delivers solute but blocks particles) was made between channels by projection lithography. Reproduced with permission from ref.[45] Copyright 2015 American Chemical Society. (c) CO_2 concentration gradient is formed in the liquid channel by diffusion of CO_2 through the PDMS wall. Reproduced with permission from ref.[48] Copyright 2017 Nature Portfolio.

experiment is $O(0.01\text{-}1)$ mm, and the observation windows do not detect the length scale on which theoretical models (equations (1)-(4)) are established ($= \lambda_D$).

Development of microfluidics boosted experimental research of diffusiophoresis in the past decade. The first microfluidic demonstration of diffusiophoresis was performed in the flow-focusing (co-flow) geometry.[28,29] In the flow-focusing systems, by varying the flow rates of different inlet channels, widths of the two liquid phases can be controlled. Abécassis et al. visualized that the salt concentration gradient across the flow streams can further change the width of the particle-laden part by diffusiophoresis (Figure 4(a)).

A microfluidic approach for establishing a concentration gradient of solute had been widely used for studies of bacterial chemotaxis,[113] prior to the appearance in diffusiophoresis studies. Concentration gradients of solutes can be set up similarly in the diffusiophoresis experiments, and thus many studies used one of the geometries shown in Figures 10-12 (some representative experimental systems are organized in Table 2).

Concentration gradient of solutes in the stream of particle suspension can be set up not only by directly contacting with the buffer solutions, but also by enabling the diffusion of solutes through permeable walls. For example, Palacci et al.[62,63] used an agarose gel based microfluidic channel (Figure 10(a)) with three separate channels to create a salt gradient

Table 2: Some common microfluidic systems used in the diffusiophoresis experiments. For detailed list of concentration gradient and the direction of particle motion (and flow) see the article by Shin.[30]

Directions	Channel Design**	System features	Other features
Solute concentration gradient and liquid flow are perpendicular to each other	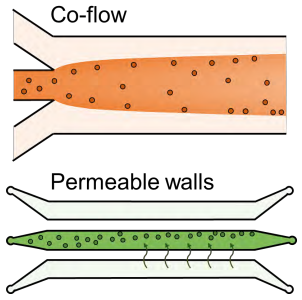	Diffusion of salt occurs within O(0.1-1) mm.[28,29,44–46,48–50,52] Steady state concentration can be obtained for solute and particles.	Ionic strength: **Salt and buffer** O(1-100) mM. **CO_2** O(10-100) μM.
Solute concentration gradient and particle motion are in the same direction	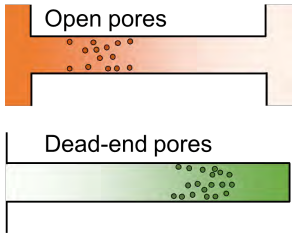	Typical pore length O(0.1-1) mm.[31,32,34,35,37,38,54,56,69,94] Steady state (e.g. open pores) or transient solute concentration and particle motion are obtained.	Diffusioosmosis along the wall influences the particle distribution by creating slip-driven flow in the pores.
Solute diffusion is in the radial direction	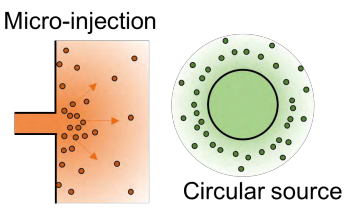	Radial diffusion of ions are obtained by micro-injection,[67] installing a circular reservoir,[39,40,85,112] or by introducing a rapidly dissolving gas (CO_2) bubble.[40]	Controlling the relative length scales of the solute source and the entire system is easy.

**Combination of two or more configurations are also reported.[85,89,112]

across the center channel, and observed diffusiophoretic focusing of colloids and DNA. Studies from the Squires' group[44–47] also utilized the three-channel configuration with an on-chip fabrication of hydrogel windows, which can let solutes diffuse between the channels. This configuration ensures symmetry in the height-direction. Shin et al.[48] used a similar configuration with a channel made with PDMS (polydimethylsiloxane), which allowed diffusion of CO_2 through the permeable walls between liquid and gas channels. For this method, if a PDMS block is bonded directly on a glass slide, the geometrical condition is analogous to the agarose gel channels. In these three-channel systems, depending on the direction or magnitudes of concentration gradients, particles showed different diffusiophoretic focusing or exclusion behaviors.

One-dimensional concentration gradient of solutes allows simpler analysis and visualization of diffusiophoresis. As introduced in the earlier section, a stable (transient) solute gradient can be generated in the dead-end pore geometry without any imposed liquid flow along the pores. Dead-end pores will be discussed in more detail in the next section. Another one-dimensional system is called the bridge or H-channel configuration (Figure 11(a)). In this system, a steady-state concentration gradient of solutes can be achieved between two reservoirs. Also, by tuning the pressures of two main channels, pores with either no-flow or flow condition can be obtained.[53,56,114] In the study by Rasmussen et al.[56] for measuring the size and charge of the vesicles, H-channels with linearly varying pore widths were used. Depending on the direction of the solute concentration gradient, diffusioosmotic velocity along the pore walls and the liquid flow inside the pores can be further controlled.

Some studies used a one-dimensional concentration gradient in the radial direction by using a circular Hele-Shaw configuration[39,40] (Figure 3(c) and Figure 11(b)). In the study by Shim et al.,[40] a CO_2 source was introduced in a circular Hele-Shaw cell in the form of a dissolving bubble or a CO_2-pressurizing chamber (with PDMS walls). Then the motion of polystyrene particles and bacterial cells was observed near the CO_2 sources with moving or fixed boundaries. Banerjee et al.[39] used projection lithography (UV curing of PEG-DA

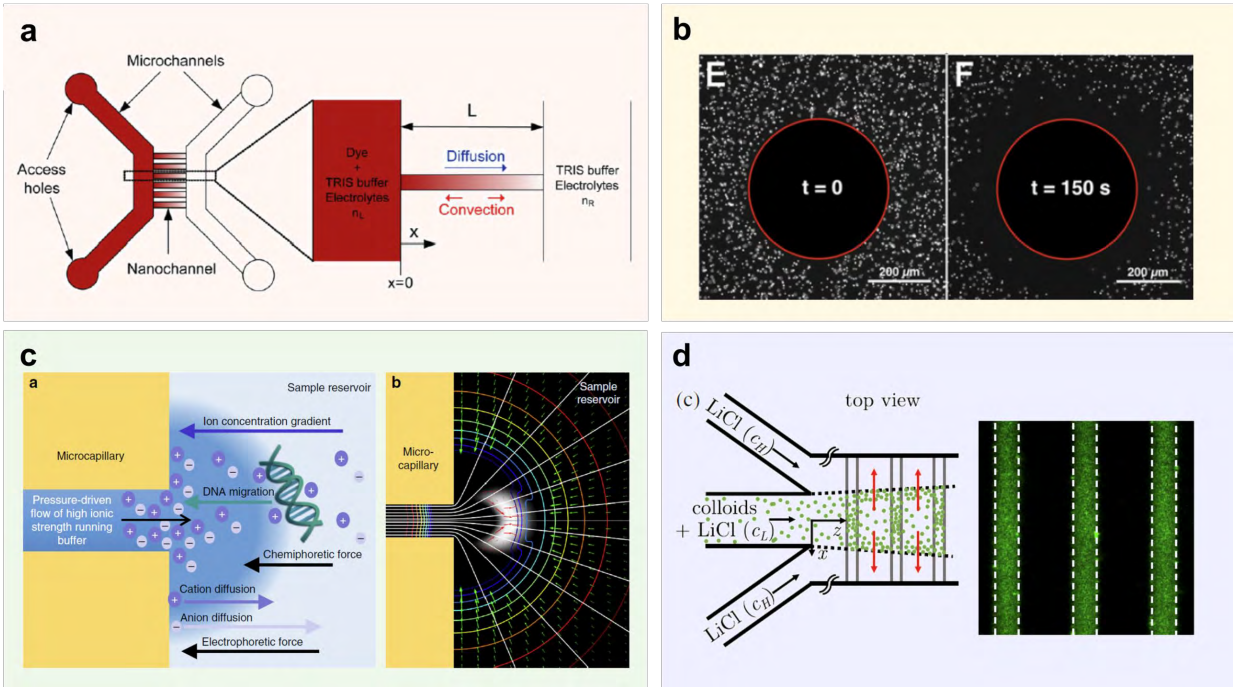

Figure 11: Multiple ways to set up solute concentration gradients in microfluidic systems. (a) H-shaped channel with two reservoir channels, which can set up a steady concentration gradient along the open pores. Reproduced with permission from ref.[53] Copyright 2014 American Physical Society. (b) Soluto-inertial beacon made by on-chip projection lithography. Reproduced with permission from ref.[39] Copyright 2016 National Academy of Sciences. (c) Micro-injection creating a radially diffusing solute profile in the large channel. Reproduced with permission from ref.[67] Copyright 2017 Nature Portfolio. (d) Mixed configuration with the co-flow and microgrooves. Reproduced with permission from ref.[89] Copyright 2020 American Physical Society.

hydrogel) with a circular photomask to generate a circular "beacon", which served as an electrolyte reservoir. Diffusiophoretic migration of polystyrene particles are measured by their velocities. Another way to create a radial concentration gradient is micro-injection (Figure 11(c)).[66,67] In this system, the injection is done by pressure-driven flow, and thus the advective component can be adjusted for additional control of the solute flux. Diffusiophoretic accumulation of DNA was observed near the injection outlet.

Lastly, a combination of co-flow and dead-end pore (microgroove) configurations is reported by Singh et al.[89] for reversible trapping of particles (Figure 11(d)). By introducing a steady-state concentration gradient of LiCl in the flow-focusing main channel, the authors obtained trapping of polystyrene particles inside the inlet of the grooves, which are located at the bottom wall of the main channel. Particles were not trapped without any salt concen-

tration gradient, and the trapping was reversible by flipping the direction of concentration gradient. Such ideas can inspire new ways to transport particles in a solute gradient by appropriately modifying the flow structure.

As described with multiple systems, different geometries can create various concentration gradients of solutes and drive the motion of particles. In microfluidic channels, due to the charged nature of typical wall materials, setting up a concentration gradient naturally creates diffusioosmosis along the walls. Typical wall materials like glass, PDMS, or PMMA (polymethylmethacrylate) have similar surface potentials with the commonly used particles like polystyrene, silica, etc.,[74,77,79] which means that the order of magnitude of the diffusioosmotic slip velocity and particle velocity are comparable. This is an important issue in the microfluidic analyses of diffusiophoresis, because diffusioosmotic slip affects the local flow structure, which is included in the detected particle motion. Particles at different positions will experience different flow velocities induced by the wall diffusioosmosis, so the resulting collective transport deviates from what can be predicted by the diffusiophoresis-only analysis.

The influence of diffusioosmosis is one of the complications that can arise in microfluidic systems. In the following sections, by further reviewing the dead-end pore and the channel flow configurations, I will discuss the one-, two-, and three dimensional features of the system and their contributions to the experimental observations of diffusiophoresis.

5.1. Two-dimensional effects on one-dimensional analysis

A dead-end pore has been used to demonstrate various transport behaviors along a one-dimensional solute gradient (Figure 12).[31–38,69,75,84,94,115–118] As described above, H-shaped channels with open-end pores can also generate one-dimensional concentration gradient of solutes. In the H-channel, a steady-state concentration gradient can be set up, which generates constant diffusioosmotic velocity along the wall. By controlling the pressure difference between two reservoir channels, additional flow velocity can be imposed on top of the

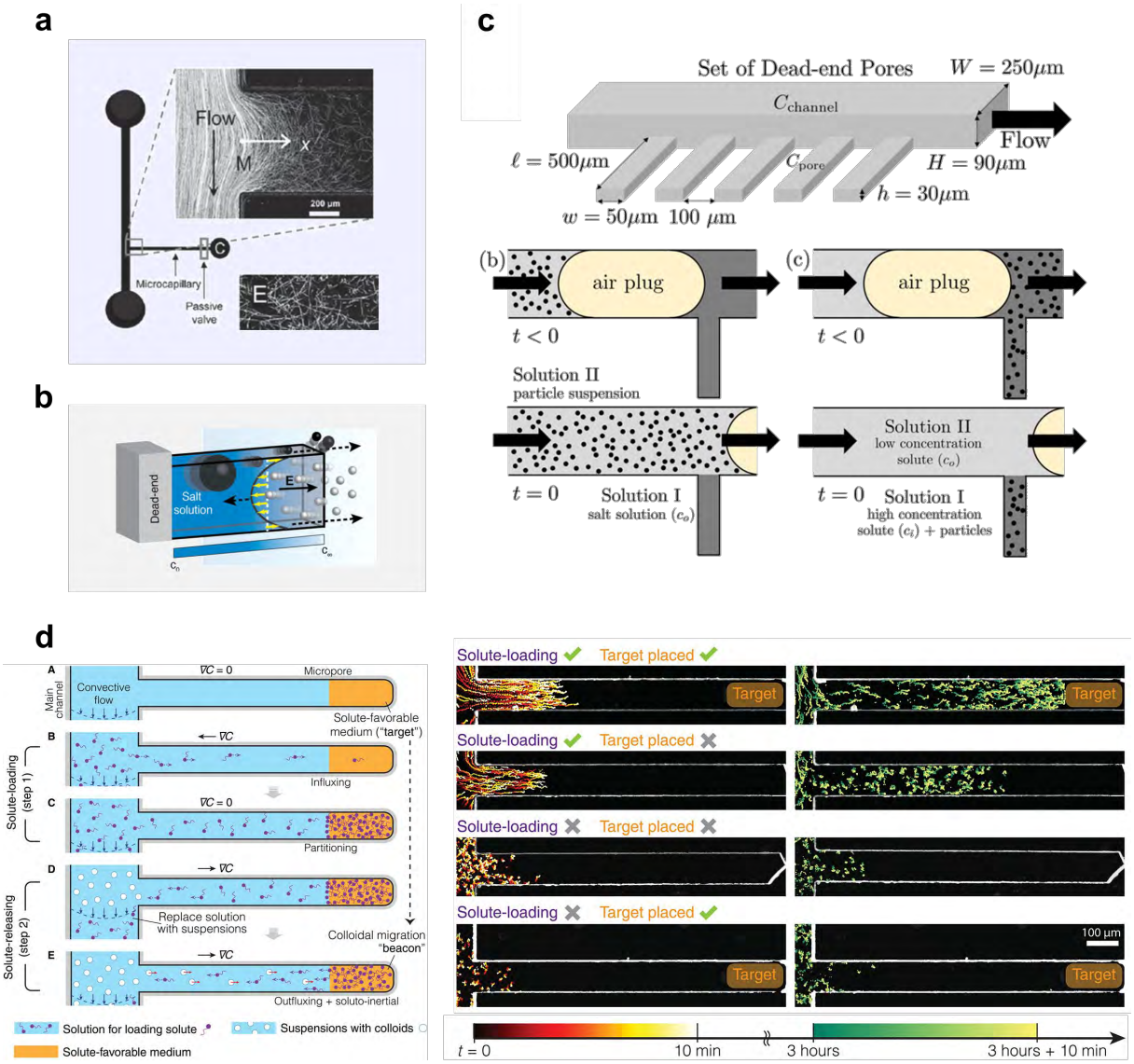

Figure 12: The dead-end pore geometry. (a) T-shaped channel with a passive valve at the end of the pore (or the narrower channel). Reproduced with permission from ref.[115] Copyright 2008 Cell Press. (b) Dead-end geometry formed with glass capillaries. Reproduced with permission from ref.[31] Copyright 2015 American Chemical Society. (c) Multiple-pores in a row, and schematics explaining entrainment and compaction experiments. Reproduced with permission from ref.[37] Copyright 2020 American Chemical Society. (d) Two-step target delivery in dead-end pores using diffusiophoresis. Reproduced with permission from ref.[116] Copyright 2021 American Association for the Advancement of Science.

diffusioosmotically-induced flow. Mathematical treatment for the leading-order analyses of these quasi-one-dimensional systems are analogous,[55,114] and thus I discuss the dead-end pore only.

In the microfluidic dead-end pore systems, one electrolyte solution is first filled in the

pores, then followed by an air bubble, the second electrolyte solution is flowed in the main channel and it comes in contact with the liquid in the pores. If the particles are introduced in the system with the second liquid, they can entrain in the pores by diffusiophoresis; or if the particles were initially trapped in the pores with the first electrolyte, then they can either compact or leave the pore by diffusiophoresis after the second solution is connected (Figure 12(c)).

The one-dimensional advection-diffusion equation for the particle concentration n is then

$$\frac{\partial n}{\partial t} + \frac{\partial (u_p n)}{\partial x} = D_p \frac{\partial^2 n}{\partial x^2} \ , \quad \text{where} \quad u_p = \Gamma_p \frac{\partial \ln c}{\partial x} \ , \tag{9}$$

and the solute concentration field can be obtained by solving the diffusion equation, $\frac{\partial c}{\partial t} = D_a \frac{\partial^2 c}{\partial x^2}$. Note that the advective contribution of the bulk liquid flow (in the pore) is neglected in the one-dimensional analysis. For a constant surface potential of the particles and negligible λ_D, a constant Γ_p can be assumed, and the particle distribution is obtained by applying appropriate boundary conditions. Both in particle entrainment and compaction configurations, a local peak in the distribution can be identified, and the peak propagation along the pore indicates the diffusiophoretic velocity $u_p(x,t)$.

Similarity transform can give insights for early time peak propagation (or for a semi-infinite pore) by defining $\eta = \frac{x}{\sqrt{4D_a t}}$. Consider the similarity transform of the characteristic line $\hat{\eta}(t) = \hat{x}(t)/\sqrt{4D_a t}$, then the definition $\dfrac{d\hat{x}}{dt} = u_p(\hat{x},t) = \Gamma_p \dfrac{\partial \ln c}{\partial x}$ can provide information of peak propagation. In the particle entrainment case, the propagating front can be approximately described by (for $\Gamma_p \ll D_a$)[119]

$$\hat{\eta} = \sqrt{\frac{\Gamma_p}{2D_a}} \ \text{ for } \ \Gamma_p > 0 \ \text{ and; } \ \hat{\eta} = -\frac{\Gamma_p}{D_a\sqrt{\pi}} \ \text{ for } \ \Gamma_p < 0 \ . \tag{10}$$

In experiments, the influence of diffusioosmosis[31,42,120] is acknowledged, but since the no-net-flux condition makes the one-dimensional (1D) characterization of the peak unperturbed by the wall diffusioosmosis, the 1D model (equation (9)) is conveniently used to analyze

particle diffusiophoresis[32,35,37] in the dead-end pores. However, if the analysis of the phenomenon as a whole including the flow field is desired, two- or three-dimensional model is necessary.

Alessio et al.[38] presented diffusiophoretic compaction of polystyrene particles in the two-dimensional (2D) pore, and directly compared with the two-dimensional representation of the experimental data (Figure 13). The study included effects of multiple ions, so the diffusiophoretic velocity of particles and the diffusioosmotic slip along the walls are calculated using equation (4). Considering the mass conservation along with the lubrication approximation

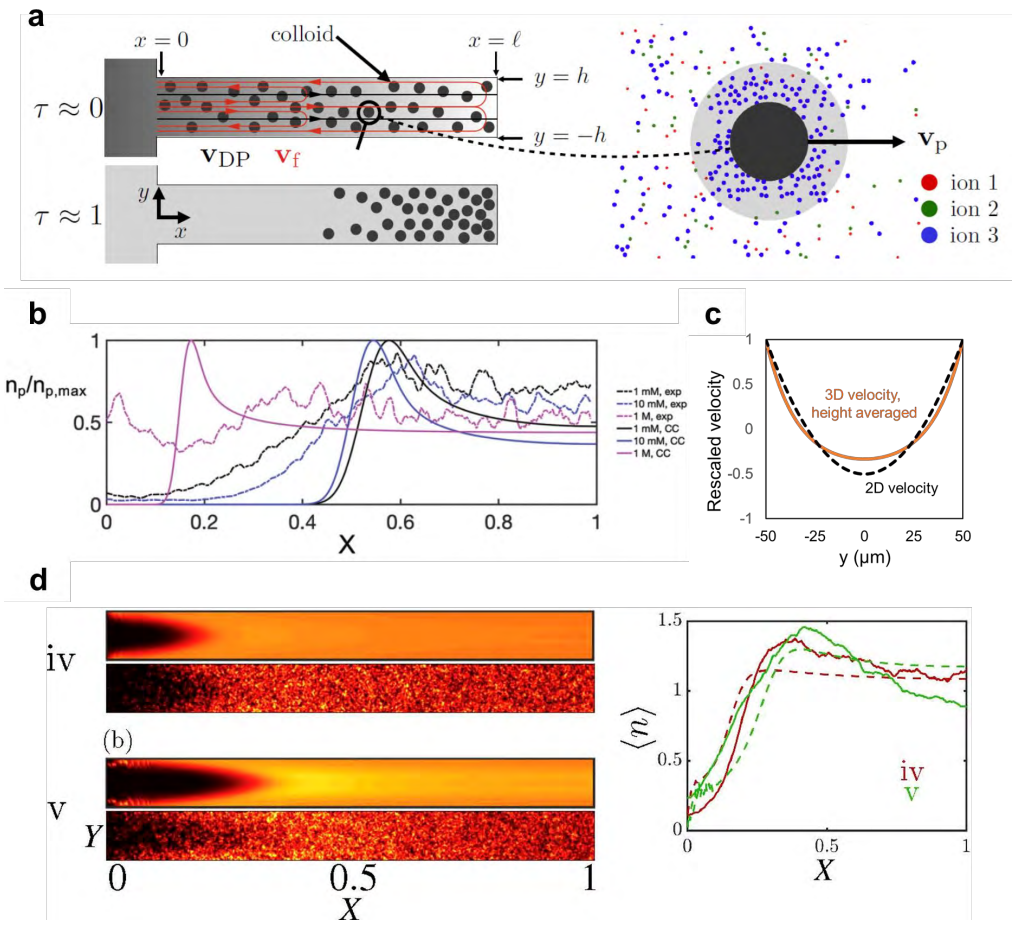

Figure 13: (a) Schematic of a two-dimensional pore system. (b) Comparison between experiments and one-dimensional calculations. Reproduced with permission from ref.[35] Copyright 2020 Royal Society of Chemistry. (c) Flow velocities (rescaled by u_{do}) obtained by 2D and 3D calculations. (d) Two-dimensional compaction of polystyrene particles induced by different ion concentration gradients. (10 mM NaCl & 10 mM KCl pair and 1 mM NaCl & 1 mM KCl pair; Details in ref[38]). (a,d) Images reproduced with permission from ref.[38] Copyright 2021 American Physical Society.

in the long, narrow pore ($h \ll \ell$), two-dimensional flow velocity is obtained as a function of the slip velocity $v_s(= u_{do})$; and the particle distribution is solved using two-dimensional advection-diffusion equation (equation (9) in 2D). The Péclet number for the solute scales as $Pe_s \approx \frac{u_{do}\ell}{D_a} \approx \frac{\frac{\Gamma}{\ell}\ell}{D_a} = \frac{\Gamma_w}{D_a} < 1$, and for diffusiophoretic particles $Pe_p \approx \frac{u_{do}\ell}{\Gamma_p} \approx \frac{\Gamma_w}{\Gamma_p} \approx 1$. Therefore, it is right that the dead-end pore geometry is a good tool for setting up a one-dimensional concentration gradient. However, for particles, including the two-dimensional effects can better predict the distribution achieved by combination of diffusiophoresis and diffusioosmsis.

The three-dimensional flow structure must be considered for the cases where 3D effects are important (e.g. dispersion of particles in the pore, inlet region, 3D particle tracking, etc.). Moreover, since diffusiophoresis is a relative motion of particles to the fluid motion, when performing exeprimental analyses, it is crucial in general that the detected particle motion is not confused with the transport by the local flow.

5.2. Main channel flow in dead-end pore experiments

Microfluidic dead-end pore experiments are initiated with a simple attempt for testing the one-dimensional transport. In the presence of a solute concentration gradient, we now know that diffusioosmosis generated along the walls creates liquid flow inside the pores. The liquid flow influences particle distribution along the pore, so clearly there is complication due to this slip-driven flow. At the inlet of the pores, there is another source of complication, which is the circulating flow that is generated by the flow in the main channel.

Battat et al.[34] reported diffusiophoretic entrainment of particles in the dead-end pore geometry and observed that there is always penetration of streamlines at the inlet region of the pores (Figure 14(a)). The configuration is similar to that of the driven cavity flow systems (lid-driven cavity flow or flow past a cavity).[121–123] In the model studies for diffusiophoresis in dead-end pores, the pore inlet is conveniently assumed as a flat boundary with zero velocity, and the influence of the shear-driven flow is not included.

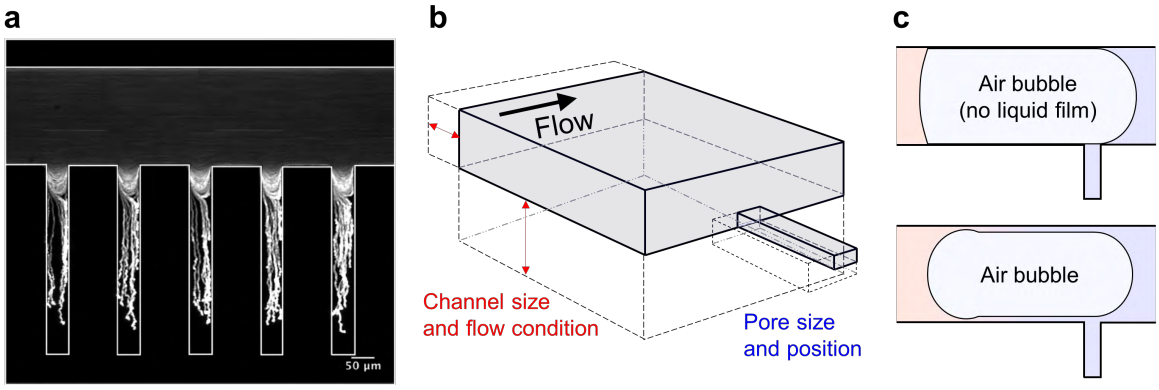

Figure 14: Pore inlet region in the dead-end pore experiments. (a) Penetration of streamlines at the pore inlet due to the main channel flow. Reproduced with permission from ref.[34] Copyright 2019 Royal Society of Chemistry. (b) Schematic showing designs of main channel and a pore. (c) Schematic showing different shapes of the air bubble flowing in the main channel and liquid film surrounding the bubble.

Depending on how the channel is designed (Figure 14(b)) and how the flow is set up in the main channel, the inlet region flow will have different forms. Relative sizes of the main channel and the pores, the aspect ratios of the main channel and pore (inlet) cross-sections, and the location of the pores all influence the shape of the streamlines that penetrate the pore inlet. In most studies that used dead-end pores, primary analyses do not include both the inlet and the dead-end regions of the pores. However, if the observation is localized near the pore inlet or if the diffusiophoretic mobility is not large enough so that the particles do not escape the inlet region by diffusiophoresis, inclusion of the complex flow behavior on the particle analysis is necessary. Pores with irregular shapes or small depths may also be influenced by how the boundary conditions are set up at one end of the pores. Note that the flow at the inlet region also affects the solute transport in the pores.

One last thing to mention about possible complication in diffusiophoresis analysis is related to how we set up the concentration gradients. In many microfluidic systems made for studying diffusiophoresis, often two different solutions are separated by an air plug or a stream of immiscible liquid. In the example of the dead-end pore experiments (Figure 14(c)) using an air bubble, the second liquid followed by the air plug merges with the first liquid abruptly at the pore inlet. Then such sharp pressure change at the inlet region may introduce

additional convective component to the solute transport and particle motion. Formation of air bubbles or oil droplets at the main inlet of the system, their flow along the channel, and their interactions with the liquid in the pores can vary depending on the inlet condition, Capillary number of the main channel flow, channel geometry, etc.[124–128] Of course, one can only care about the result of diffusiophoretic transport if diffusiophoresis dominates all other factors in the system, but again, it is always important to be aware that particles move in the fluid, and an unexpected fluid motion can be generated by the activity of setting up the experiments.

5.3. When channel walls have other contributions

Next, I will discuss the system where diffusiophoresis of particles are observed without any pre-imposition of the solute gradient. Thus this section is about formation of an unexpected concentration gradient in the system. Shim and Stone[59] reported findings about spontaneous particle accumulation in the channel flow, which occured by simply turning on the flow. After the molding technique using photoresist (e.g. SU-8) became common, the term "standard soft lithography" represents the method for making a PDMS channel. Given a simple geometry (a single stream channel), a PDMS channel refers to the pattern engraved on the PDMS block, which is bonded on a glass slide. Liquid of interest can be injected into the channel by using a syringe and a connecting tube (Figure 15).

In this simplest configuration, a dilute suspension of amine-modified polystyrene particles (a-PS; positively charged in water, $d = 1$ μm) showed an unexpected focusing as it flowed

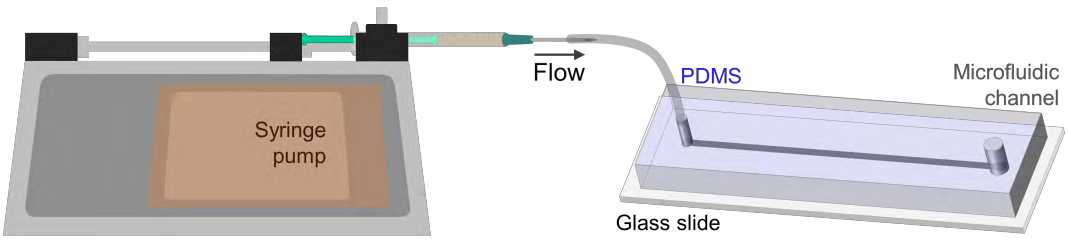

Figure 15: Schematic of a typical setup with a PDMS microfluidic channel connected to a syringe.

into the channel. The focused patch of particles then flowed downstream with the liquid stream. The accumulation behavior was charge-dependent (negatively charged PS particles behaved differently), and was completely suppressed in the systems made with non-permeable materials (UV curable epoxy and glass).[59] The accumulation of positively charged particles (a-PS) was referred to as a "pulse", of which the speed was measured to unravel the physical mechanism.

In the PDMS channel and the aqueous particle suspension, there is small amount of gas that is pre-dissolved by being in equilibrium with the atmospheric condition. Such tiny amount of species can have large impact on the main event of interest in small scale systems.[129] In the experiments by Shim and Stone,[59] by turning on the flow, a nonzero pressure gradient is built up across the PDMS walls (largest near the inlet), inducing CO_2 leakage through PDMS. Therefore, a local concentration gradient of CO_2 forms across the channel, and diffusiophoretically accumulate the particles. Positively charged particles focus toward the high-CO_2-concentration region, whereas negatively charged polystyrene particles

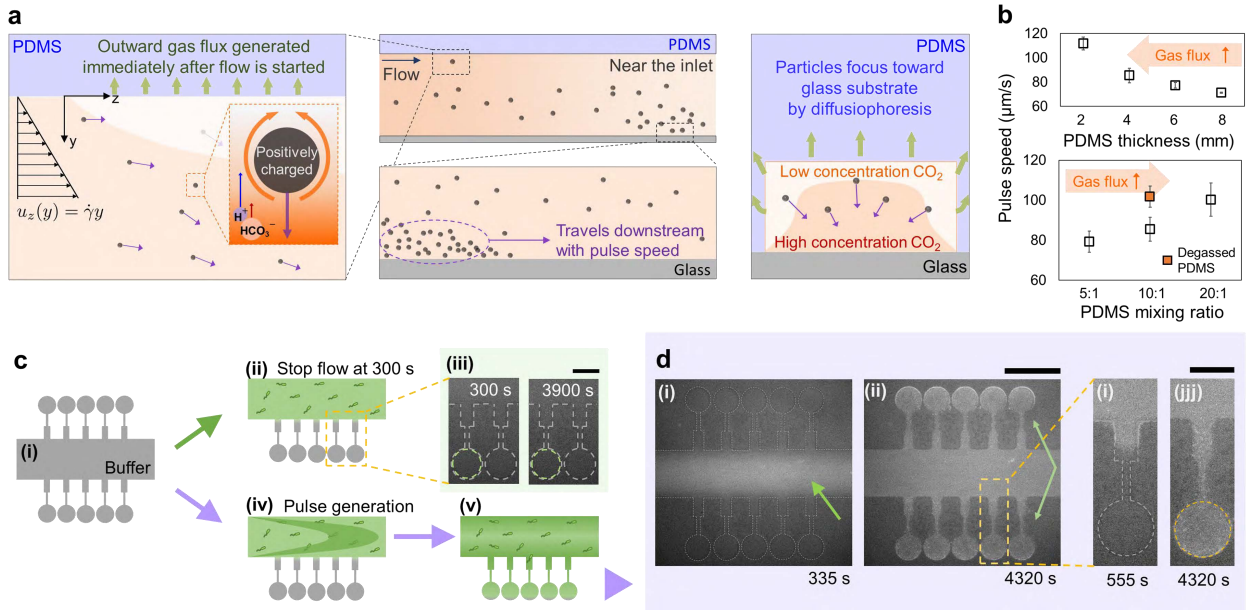

Figure 16: Spontaneous pulse generation in channel flow. (a) Schematics for the hypothesis of CO_2-leakage-driven diffusiophoresis. (b) Pulse speed measured for different gas fluxes in PDMS. (c,d) Use of pulse generation for protein separation. Images adapted from ref.[59] Copyright 2020 National Academy of Sciences.

move toward the PDMS walls, where the CO_2 concentration is low (Figure 16).

The reported pulse speed had consistent trends with the gas permeability of PDMS, and thus confirmed that the particle accumulation is due to the leakage of gas. The authors further investigated the flow of a bacterial suspension. The system had cells and fluorescent protein (mKO) in the background medium, and by creating a pulse, the mKO molecules which are estimated to be positively charged at pH $\approx$ 6-7 were separated from the cell suspension.

The study suggests that in common microfluidic systems, an unintended concentration gradient of solute can form and create diffusiophoresis of charged particles. Not only for the protein separation, but the phenomenon has various potential applications, because particles accumulate near the inlet depending on their surface charge. Therefore, by flexible designs of the channels, such focused particles can be used for other analyses in separation, phoresis, or dispersion systems.

5.4. Three-dimensional effects on two-dimensional systems

The directional transport of particles by diffusiophoresis motivated practical research, by applying the phenomenon to water cleaning systems (Figure 17). Shin et al.[48] (CO_2-driven diffusiophoresis), Lee et al.[50] and Seo et al.[52] (Nafion) reported in-flow particle separation systems, by creating the concentration gradient of ions using the ion source on one side wall. The configuration has the feature of field-flow fractionation,[130–132] and thus the diffusion potential across the flow induces particle separation by diffusiophoresis.

In each study, diffusiophoresis of a-PS and PS particles, bacterial cells (*E. coli* and *S. typhimurium*), and c-PS particles are demonstrated, respectively. Also, Lee et al.[50] provided a scaling argument for the particle exclusion zone (EZ) that the size (δ) of the EZ follows the relation $\delta \propto (U/w)^{-\frac{1}{3}}$, where U, w, are respectively, the mean flow speed and the width of the channel. U/w is the two-dimensional estimation of the wall shear rate $\dot{\gamma}$. For practical purposes, achieving a controlled particle separation in a wide range of length scales

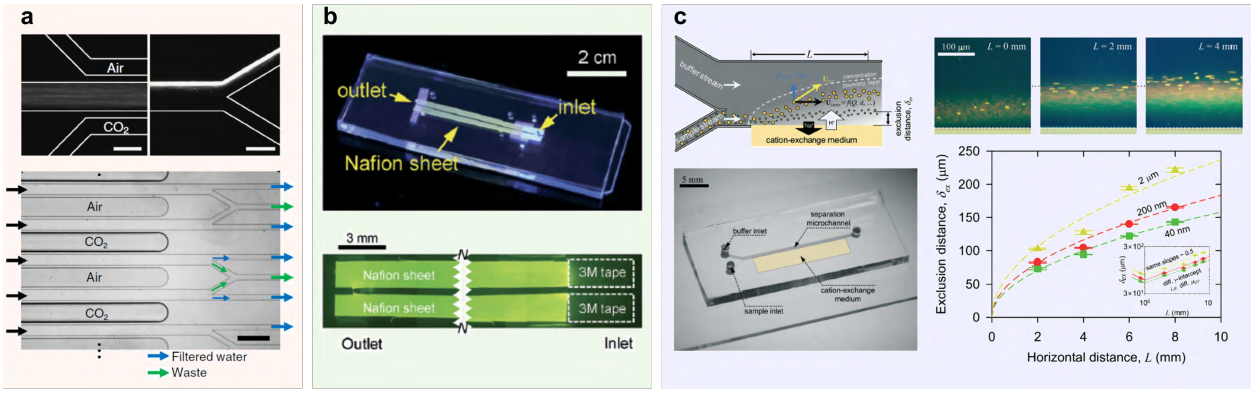

Figure 17: In-flow particle separation systems. (a) CO_2-driven diffusiophoresis for membraneless filtration. Reproduced with permission from ref.[48] Copyright 2017 Nature Portfolio. (b,c) Separation of particles in the channel with Nafion wall(s). (b) Reproduced with permission from ref.[50] Copyright 2018 Royal Society of Chemistry. (c) Reproduced with perimission from ref.[52] Copyright 2020 Royal Society of Chemistry.

is helpful. However, this is not simple, because of the non-linearity of diffusiophoresis and diffusioosmosis. This configuration is a good example that visualizes complicated geometric dependence of diffusiophoresis experiments.

Shim et al.[49] studied the geometry in more detail by considering the flow structure and different length scales; and by applying shear flow approximations. A two-dimensional channel view where the CO_2 source is located at $y = 0$ along the x-axis is first considered. For a small region near the wall where the solute source is located, a shear flow can be assumed and Lévêque problem-like analysis[133,134] can be done by further applying the boundary layer approximation. Then the analyses using similarity transform suggests a critical similarity variable η_c, which is a measure of the particle exclusion zone for negatively charged PS particles (as deduced by Lee et al[50] and mentioned above):

$$\eta_c = \frac{y_c}{\left(3x_c \frac{D_c}{\dot{\gamma}}\right)^{\frac{1}{3}}} \ . \tag{11}$$

(x_c, y_c) are the coordinates of the boundary of the EZ, and D_c is the CO_2 diffusivity in water. Therefore, the shape of the boundary layer can be estimated as $y = \alpha\eta_c(3x(D_c/\dot{\gamma}))^{\frac{1}{3}}$, where α is a prefactor. The two-dimensional wall shear-rate $\dot{\gamma}$ in this study is calculated using

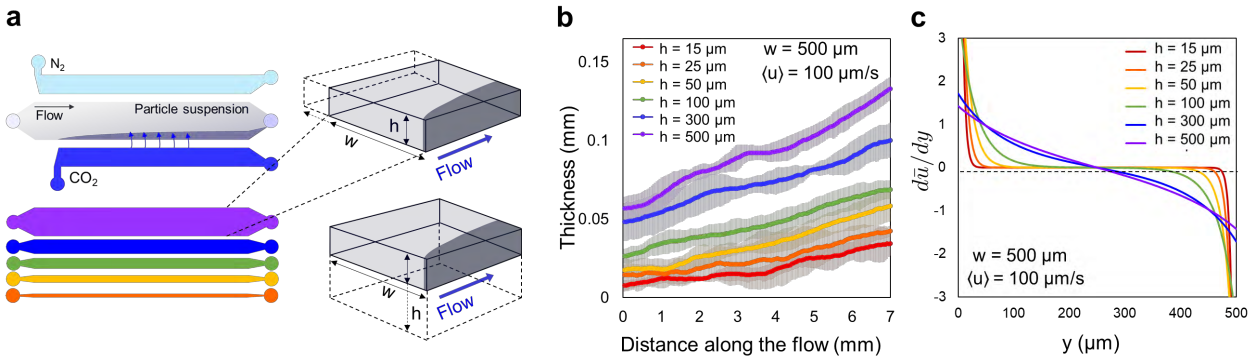

Figure 18: (a) Schematic of multiple-length-scale experiments. (b) Exclusion zone measurements done in channels with different heights at the same width and mean flow velocity. (c) 2D shear rates calculated from the 3D velocity profiles. Images adapted with permission from ref.[49] Copyright 2021 Royal Society of Chemistry.

the height-averaged velocity profiles ($\bar{u}$) of the three-dimenional rectangular channel flow. Considering the 3D effect, the shear rate becomes a function of the mean flow speed and both the width (w) and height (h) of the channel ($\dot{\gamma} = f(\langle u \rangle, w, h)$)[49] (Figure 18)). Note that the boundary shape estimation $y = \alpha\eta_c(3x(D_c/\dot{\gamma}))^{\frac{1}{3}}$ has the same shear rate dependence with the relation derived by Lee et al.[50] ($\delta \propto (U/w)^{-\frac{1}{3}}$), but the detailed shear rate calculations suggest that two-dimensional analysis does not fully capture the flow effect, and thus it is difficult to provide criteria for the system scalability.

Shim et al.[49] further examined numerically the effect of diffusioosmosis along the top and bottom walls for the no-flow condition, and showed that the influence of diffusioosmosis on the height-averaged (z-averaged) particle distribution is small. This may explain the good agreement between the 2D diffusiophoresis model and experiments reported for the steady, co-flow system by Abécassis et al.[28,29]

As described in the three different configurations (dead-end pores, permeable PDMS channels, in-flow separation systems), there can be always unexpected complications set by the flow in microfluidics for diffusiophoresis. Therefore, the analyses for particle motion have to be accompanied by the understanding of the flow structure. Such careful and thorough approaches will fill the large gap between the typical scales of microfluidic experiments (e.g. $\ell = O(0.01\text{-}1)$ mm) and the typical scales over which theoretical models for diffusiophoresis

are established (e.g. $\lambda_D = O(1)$ nm).

5.5. Complex geometry and multi-scale systems

The versatility of microfluidics extends the diffusiophoresis studies from demonstration of collective particle motion to more complicated analyses and visualization. In chemotaxis studies, complicated geometries are utilized to understand the swimming and decision-making behaviors of bacterial cells.[113,136] A similar approach has been investigated by Gandhi et al.,[90] where the path choice and transport time of colloidal particles were analyzed in the T-junction and corners located between two reservoir channels (Figure 19(a)). The width of the paths is 5 μm, which is comparable to the particle diameter (1 μm). Numerical analysis is made for different chemical-gradient response of particles (different dependences on ∇c), and the authors report that the path selectivity is improved for larger particles. However, when a run-and-tumble dynamics is considered for the particle navigation, the behavior was similar to that of simple diffusion, confirming that the run-and-tumble dynamics is different from the diffusiophoretic migration along the gradient of solute. This result may be consis-

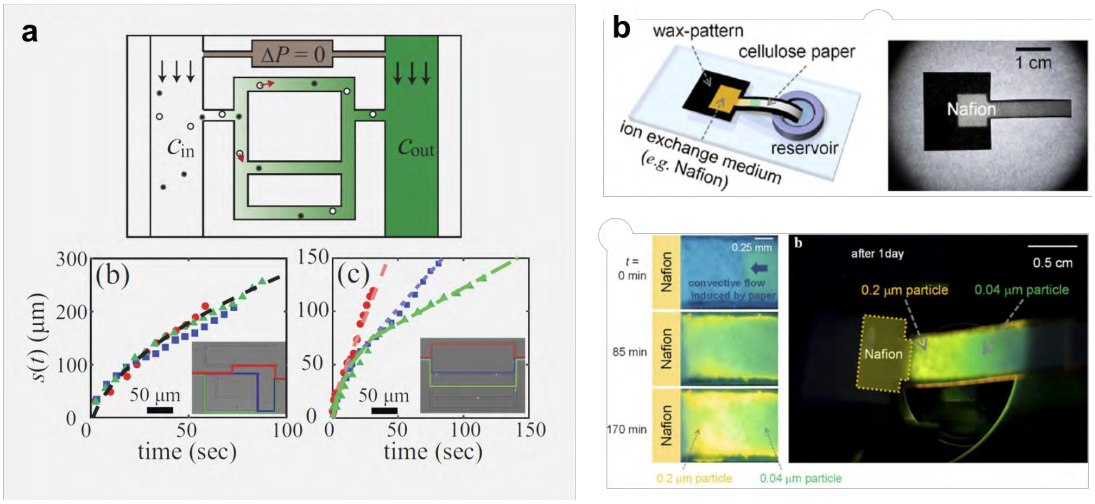

Figure 19: (a) Path selection of particles in the concentration gradient along the pores. Reproduced with permission from ref.[90] Copyright 2020 American Physical Society. (b) Diffusiophoretic separation of particles in the paper-based microfluidic device. Reproduced with permission from ref.[135] Copyright 2020 SpringerOpen.

tent with the observation by Shim et al.[40] on the separate mechanism of random bacterial swimming and diffusiophoresis.

Lee and Kim[135] reported a counterintuitive separation of polystyrene particles (c-PS) in a paper-based microfluidic system (microfluidic paper-based analytical device; μPAD). The mechanism is similar to the system reported in ref.[51] where ion exchange and imbibition of liquid through Nafion induced diffusiophoretic transport of particles. However, in the μPAD system, the authors observe the opposite separation of the particles of two different sizes ($d = 0.2$ μm and $d = 0.04$ μm) that cannot be explained by the diffusiophoretic mobility only (Figure 19(b)). Complex geometry of cellulose (average pore size 11 μm) may contribute to the results due to the pore-particle interaction and slightly charged nature.

A recently published study discusses amplified diffusioosmotic flows (DO) in nanoporous systems[137] (Figure 20). The authors report methods to create nanoscale porous system inside a microfluidic channel by packing nanoparticles (SAPM; self-assembled particle membrane). When a concentration gradient of salts are imposed across the porous system at different temperatures, diffusioosmotic flow is generated along the pore surfaces. Such diffusioosmotic flow is measurable and larger than that created along a single pore. Although performed at different length scales, it can be speculated that the enhanced diffusioosmosis in a complex network could be one cause for the opposite separation of different-sized particles in the above paper-based system (if the walls and the particles have the same sign of the surface

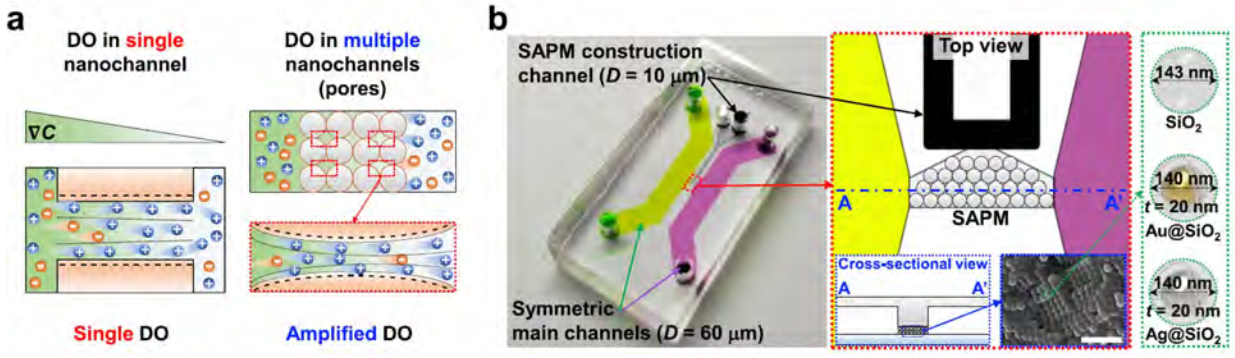

Figure 20: Enhanced diffusioosmosis across a nanoporous system. Reproduced with permission from ref.[137] Copyright 2021 American Chemical Society.

potential).

Other example of complex geometry is the system with multiple scales. Hong et al.[70] and Ha et al.[61] report diffusiophoresis of charged particles in the combined micro- and nanopore geometries (Figure 21). In the two studies, the nanopores connected to the micro-channel were used to set up the concentration gradients in the microfunnels[70] and micropores,[61] respectively. Such separation in the length scales allows solutes to freely diffuse in the nanopores, with either a controlled or a zero flow condition maintained due to high hydraulic resistance.

In the PMMA channels with microfunnels connected to the nanopores (Figure 21(a)), a single particle- and cell-level manipulation was achieved. The authors report trapping of a single charged particle in the 3D microfunnel region by diffusiophoresis, and show that the method can be used to trap *E. coli* cells. Such method can be useful for single cell analysis systems. In the study by Ha et al. (Figure 21(b)), the nanopore was made by cracking-assisted photolithography. The geometry allows in-situ manipulation of charged particles by

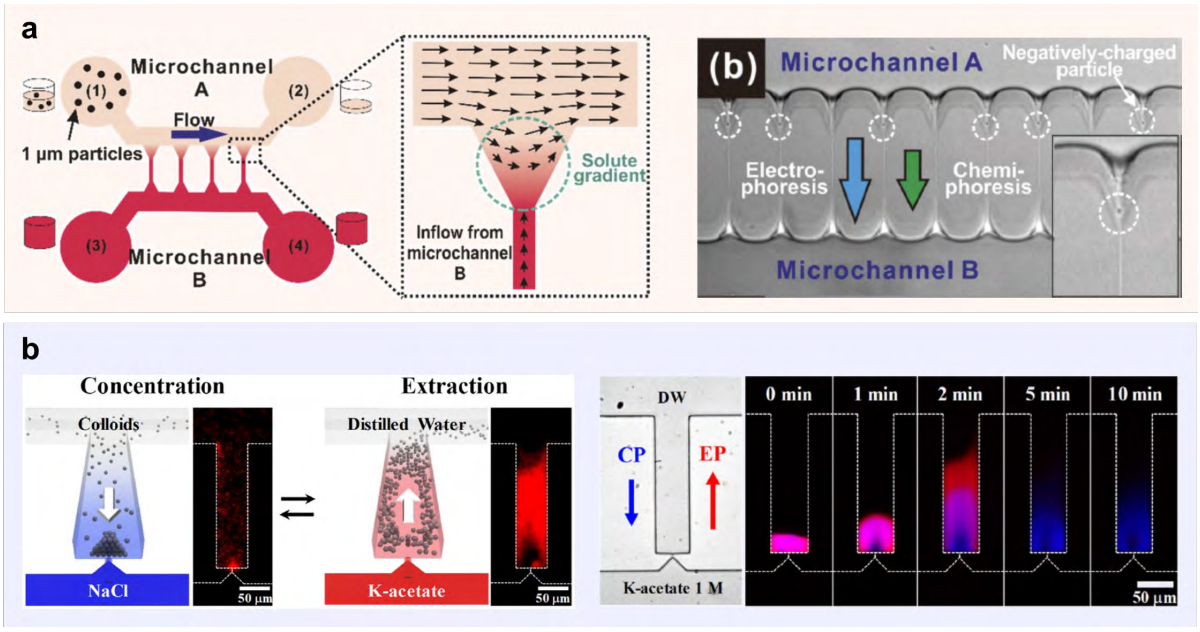

Figure 21: Systems with mixed scales. (a) 3D microfunnels between two reservoir microchannels, bridged with nanopores. Reproduced with permission from ref.[70] Copyright 2018 Royal Society of Chemistry. (b) Crack-end pores where a micropore is connected to the reservoir by a nanopore. Reproduced with permission from ref.[61] Copyright 2019 American Chemical Society.

refreshing the concentration gradients through the nanopore-connected reservoirs, without generating unwanted leakage of particles or liquid from the micropores. Such configuration shows analogous features to the dead-end pore geometry, but has more flexibility in terms of transient controls.

Fabrication of the combined micro-nano systems require advanced technique and strict control of materials. Also, as the length scale decreases, additional consideration of electrokinetics is required to include higher-order influences of electrical double layers. Such complication in the diffusiophoresis systems is yet to be actively investigated, so has the potential to develop.

6. Concluding remarks and perspective

Microfluidics has been a very useful tool for visualizing diffusiophoresis and diffusioosmosis of colloidal suspensions. Many studies highlighted controllable particle transport along solute concentration gradients, assisted by model calculations that agreed well with the experimental results. For simple comparisons, diffusiophoretic mobility considering a constant surface potential with negligible double layer thickness is utilized. This analysis is a good characterization of the systems that are in moderate ranges of scales (e.g. moderate solute concentrations, particles and channel sizes, etc.).

For the system conditions where constant surface property assumptions do not apply, theoretical explanations including higher order influences were provided. Finite double layer thickness and varying surface potentials can explain that some unphysical results predicted by a simple theory (e.g. ballistic motion of particles in the region without salt) are not achievable in the real systems. Coupled ionic fluxes[118] need to be considered in the presence of three or more ions, and the valence asymmmetry can be used for enhanced or reduced diffusiophoretic mobilities.

Most studies used synthetic microspheres for controlled system chararcterization, but

there are active efforts to extend the investigation to biological materials. Phenomenological analogy of diffusiophoresis and chemotaxis motivated studies of swimming bacteria; and microfluidic size and charge measurements were demonstrated with phospholipid vesicles. Also, novel techniques for handling intracellular materials enabled validation of diffusiophoresis of cell cargo driven by minD and minE gradients. Such results suggest promising direction of the research area in the sytems with multiple length and time scales.

In microfluidic experiments, local flow structure can introduce unexpected transport effects to the particle analysis. Influence of the flow needs to be differentiated to make sure that the detected particle motion is diffusiophoresis. Studies report that diffusioosmosis along the walls can induce flow in the channels and contribute to the particle distribution. Also, permeable wall material naturally created ion concentration gradients in channel flows due to the leakage of gas, thereby spontaneously accumulate particles without any pre-imposed solute gradient. The complex nature of diffusiophoresis and diffusioosmosis makes varying of length scales complicated in some channel flows. Many experimental studies used one geometry per study, and in certain situations this may not be sufficient for obtaining a general conclusion, especially when the local flow structure is important.

After the large wave of initial demonstrations and visual validations of the phenomena, we are at the stage where deeper quantitative investigation is needed for the next steps. I do not know all the details, but based on the review, I would like to comment on potential research interests below.

6.1. More biological particles

The question of diffusiophoretic migration of biological matters had existed from early time of the research area, and the topics evolved to several branches. Diffusiophoresis of bacterial cells, protein, DNA, RNA, vesicles, etc. under the gradients of simple salt or physiological electrolytes, finding analogy and differences between diffusiophoresis and chemotaxis, and diffusiophoretic transport of intracellular macromolecules are all appropriate examples. One

can ask about nonelectrolyte systems like sugar transport in plants.

Bacterial cells, as discussed in the main text, can undergo both chemotaxis and diffusiophoresis, so differentiating two mechanisms of the cell response can be important. The model formulation may be different for the single-cell migration and collective behaviors.[102,138] Local concentration of ions like Na^+ or H^+ affects flagellar behaviors. Local pH can also affect physiology of the cells and surface potential, so careful investigation may provide better insights for unknown cell behaviors. Whether the tendency to show diffusiophoresis help the run-and-tumble behavior of bacteria or not is unknown. Cell-liquid interaction at the surface may play an important role in the characterization of the out-of-equilibrium double layer, by changing both the local liquid properties and cell surface properties.

On the other hand, acknowledging the analogy of chemotaxis and diffusiophoresis can guide potential directions for studies of diffusiophoresis. Chemical sensing behavior of bacterial cells has been investigated in microfluidic systems in various configurations, so similar approaches can be adopted for diffusiophoresis studies in terms of creating concentration gradient and detecting the particle motion.

Proteins show pH-dependent surface charge.[92] Such property can be studied or used in the diffusiophoresis context. It has been shown that a pH gradient can generate or affect the diffusiophoretic motion of particles.[46,50,139] Combination of salt gradient and controlled pH can provide platforms for separation systems. In this case, consideration of the typical ionic strength of the system can introduce interesting research questions, since slight change in the H^+ concentration can lead to a large change in the pH scale. For example, pH = 6 is achieved only by adding 1 μM of H^+ in the aqueous solution, and it means that particles with their isoelectric points near pH = 7 can show versatile diffusiophoretic responses to a small change in ionic strength (that includes H^+) of the system.

6.2. More complex geometries

The presence and influences of flow in simple geometries are relatively well understood in diffusiophoresis studies. Questions may arise for other porous structures with heterogeneity,[140,141] channels with comparable size with the particles,[142] channels with reacting walls and/or particles, porous particles, soft surfaces,[143,144] density-driven flows,[145] etc. In general, spatial and/or temporal heterogeneity (Figure 22) in the system configuration may not behave in a linear manner, especially when both diffusiophoresis and diffusioosmosis

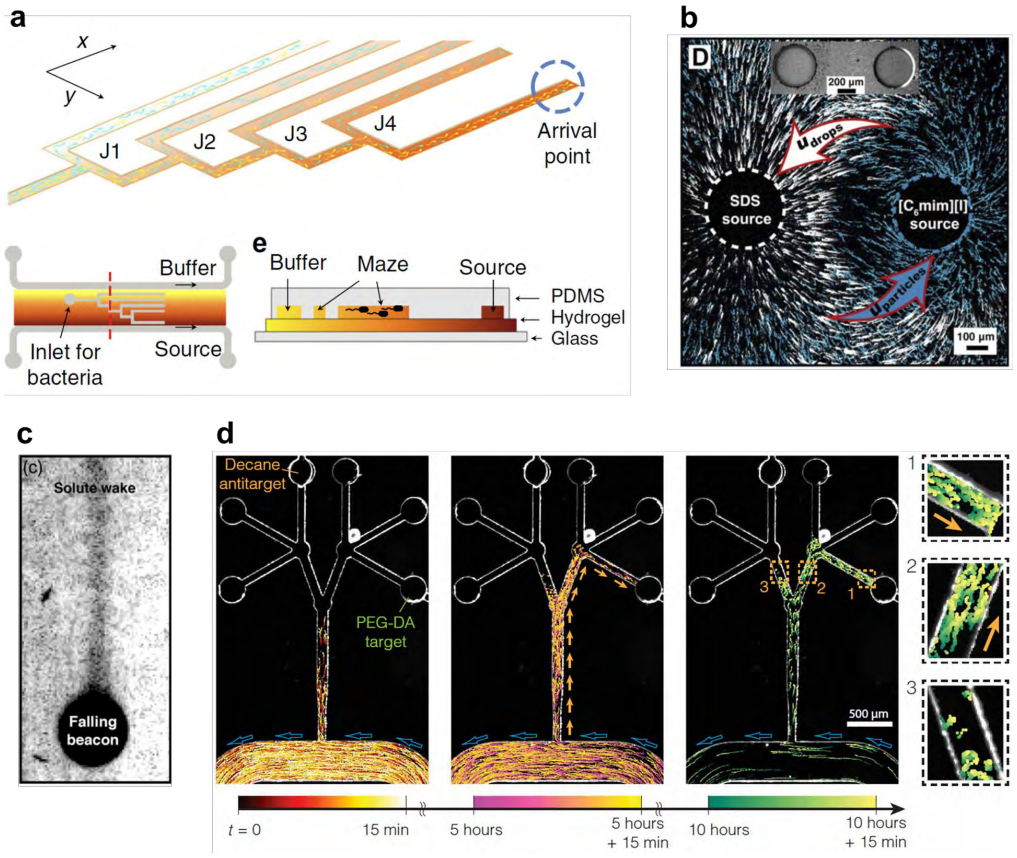

Figure 22: (a) T-maze design for choice-making study of chemotactic bacteria. Reproduced with permission from ref.[136] Copyright 2019 Nature Portfolio. (b,c) Interacting beacons and sedimenting beacon. (b) Reproduced with permission from ref.[112] Copyright 2019 American Association for the Advancement of Science. (c) Reproduced with permission from ref.[85] Copyright 2020 American Physical Society. (d) Target-delivery using diffusiophoresis in a complex dead-end pore system. Reproduced with permission from.[116] Copyright 2020 American Association for the Advancement of Science.

are present. The feature can motivate future studies for understanding the geometrical influences on diffusiophoresis and diffusioosmosis, and provide design criteria for separation, targeted delivery, water cleaning, and other practical systems.

6.3. Physicochemical hydrodynamical ingredients combined

The combination of diffusiophoresis (DP), diffusioosmosis (DO), and microfluidics is a very rich setting for physicochemical hydrodynamics research (Figure 23). Depending on the focus of the research, the phenomena can be observed as various transformations of one physical idea – concentration gradient moves particles or fluids.

I learn that this type of problems have system structures that make communications difficult between theoreticians and experimentalists, because the model considers fluid-surface interaction within the length scale of λ_D, which is an invisible, conceptual length scale for microfluidic experiments. In some situations, theories derived for a single particle may not explain how the particle is further carried by the flow set up in a channel. Experimentalists can also get blind about existing physicochemical hydrodynamical phenomena due to the resolution of the observation.

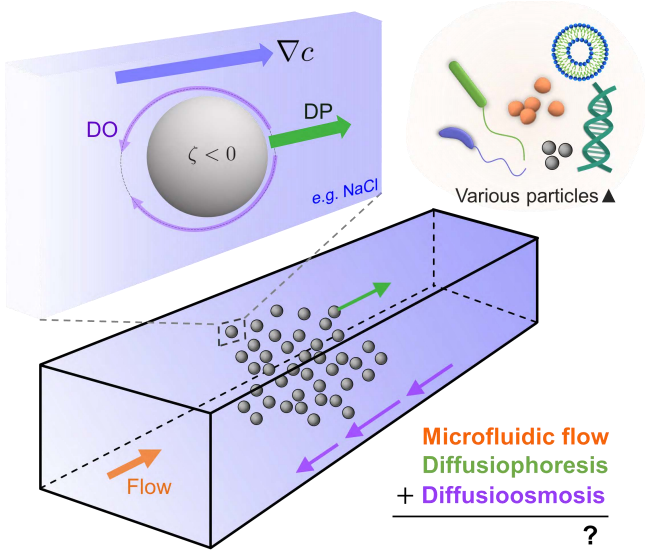

Figure 23: Schematics showing various elements of diffusiophoresis studies.

Therefore, such limitations that arise due to the default scale of interest in different communities must be acknowledged. As always, theory does not fully govern the phenomenon, and being able to suggest applications does not mean that the phenomenon is fully understood. Upon moving forward, communications among research communities is necessary for deeper understanding of fundamental and practical faces of the phenomenon.

Acknowledgement

The author thanks deeply Benjamin M. Alessio, Jesse T. Ault, Mrudhula Baskaran, Bernardo Gouveia, Ankur Gupta, Sepideh Khodaparast, Ching-Yao Lai, Bhargav Rallabandi, Orest Shardt, Howard A. Stone, Fernando Temprano-Coleto and Jessica L. Wilson for valuable discussions. We thank the NSF for support via grant CBET-2127563 (to H.A. Stone).

Biography

Suin Shim is a postdoctoral research associate at Princeton University. Suin received her B.Eng. degree in Mechanical Engineering from POSTECH (Pohang University of Science and Technology; in Pohang, Korea), and her Ph.D. in Mechanical and Aerospace Engineering at Princeton University. Her research interest is in small scale flows under various gradients, where more than one driving sources are combined to create complex behavior of fluid and other system elements. Diffusiophoresis is one good example. Suin plans to extend her expertise to unravelling many interesting (small scale) flow systems that include biological and soft matters.

Supporting Information

Video S1: Animated explanations for diffusiophoresis and diffusioosmosis in a microfluidic system.

References

(1) Derjaguin, B.; Sidorenkov, G.; Zubashchenkov, E.; Kiseleva, E. Kinetic phenomena in the boundary layers of liquids 1. Capillary osmosis. *Kolloidn. Zh.* **1947**, *9*, 335–347.

(2) Derjaguin, B.; Sidorenkov, G.; Zubashchenkov, E.; Kiseleva, E. Kinetic phenomena in the boundary layers of liquids 1. Capillary osmosis. *Prog. Surf. Sci.* **1993**, *43*, 138–152.

(3) Derjaguin, B.; Dukhin, S.; Korotkova, A. Diffusiophoresis in electrolyte solutions and its role in the mechanism of film formation from rubber latexes by the method of ionic deposition. *Kolloidn. Zh.* **1961**, *23*, 53–58.

(4) Derjaguin, B.; Dukhin, S.; Korotkova, A. Diffusiophoresis in electrolyte solutions and its role in the mechanism of film formation from rubber latexes by the method of ionic deposition. *Prog. Surf. Sci.* **1993**, *43*, 153–158.

(5) Anderson, J.; Lowell, M.; Prieve, D. Motion of a particle generated by chemical gradients Part 1. None-electrolytes. *J. Fluid Mech.* **1982**, *117*, 107–121.

(6) Anderson, J.; Prieve, D. Diffusiophoresis: migration of colloidal particles in gradients of solute concentration. *Sep. Purif. Methods* **1984**, *13*, 67–103.

(7) Anderson, J. Colloid transport by interfacial forces. *Annu. Rev. Fluid Mech.* **1989**, *21*, 61–99.

(8) Prieve, D. Migration of a colloidal particle in a gradient of electrolyte concentration. *Adv. Colloid Interface Sci.* **1982**, *16*, 321–335.

(9) Prieve, D.; Anderson, J.; Ebel, J.; Lowell, M. Motion of a particle generated by chemical gradients. Part 2. Electrolytes. *J. Fluid Mech.* **1984**, *148*, 247–269.

(10) Prieve, D.; Roman, R. Diffusiophoresis of a rigid sphere through a viscous electrolyte solution. *J. Chem. Soc., Faraday Trans. 2* **1987**, *83*, 1287–1306.

(11) Prieve, D.; Smith, R.; Sander, R.; Gerhart, H. Chemiphoresis: Acceleration of hydrosol deposition by ionic surface reactions. *J. Colloid Interface Sci.* **1979**, *71*, 267–272.

(12) Shaeiwitz, J.; Lechnick, W. Ternary diffusion formulation for diffusiophoresis. *Chem. Eng. Sci.* **1984**, *39*, 799–807.

(13) Lechnick, W.; Shaeiwitz, J. Measurement of diffusiophoresis in liquids. *J. Colloid Interface Sci.* **1984**, *102*, 71–87.

(14) Lechnick, W.; Shaeiwitz, J. Electrolyte concentration dependence of diffusiophoresis in liquids. *J. Colloid Interface Sci.* **1985**, *104*, 456–470.

(15) Ebel, J.; Anderson, J.; Prieve, D. Diffusiophoresis of latex particles in electrolyte gradients. *Langmuir* **1988**, *4*, 396–406.

(16) Staffeld, P.; Quinn, J. Diffusion-induced banding of colloid particles via diffusiophoresis. 1. Electrolytes. *J. Colloid Interface Sci.* **1988**, *130*, 69–87.

(17) Staffeld, P.; Quinn, J. Diffusion-induced banding of colloid particles via diffusiophoresis. 2. Non-electrolytes. *J. Colloid Interface Sci.* **1988**, *130*, 88–100.

(18) Pawar, Y.; Solomentsev, Y.; Anderson, J. Polarization effects on diffusiophoresis in electrolyte gradients. *J. Colloid Interface Sci.* **1993**, *155*, 488–498.

(19) Keh, H.; Weng, J. Diffusiophoresis of colloidal spheres in nonelectrolyte gradients at small but finite Péclet numbers. *Colloid Polym. Sci.* **2001**, *279*, 305–311.

(20) Ma, H.; Keh, H. Diffusioosmosis of electrolyte solutions in a fine capillary slit. *J. Colloid Interface Sci.* **2006**, *298*, 476–486.

(21) Dukhin, S.; Ul'berg, Z.; Dvornichenko, G.; Derjaguin, B. Diffusiophoresis in electrolyte solutions and its application to the formation of surface coatings. *Russ. Chem. Bull.* **1982**, *31*, 1535–1544.

(22) Smith, R.; Prieve, D. Accelerated deposition of latex particles onto a rapidly dissolving steel surface. *Chem. Eng. Sci.* **1982**, *37*, 1213–1223.

(23) Probstein, R. *Physicochemical Hydrodynamics: An Introduction*, 2nd ed.; John Wiley & Sons, Inc.: Hoboken, New Jersey, 2003.

(24) Dukhin, S. Non-equilibrium electric surface phenomena. **1993**, *44*, 1–134.

(25) Marbach, S.; Bocquet, L. Osmosis, from molecular insights to large-scale applications. *Chem. Soc. Rev.* **2019**, *48*, 3102–3144.

(26) Velegol, D.; Garg, A.; Guha, R.; Kar, A.; Kumar, M. Origins of concentration gradients for diffusiophoresis. *Soft Matter* **2016**, *12*, 4686–4703.

(27) Stone, H.; Stroock, A.; Ajdari, A. Engineering flows in small devices: Microfluidics toward a lab-on-a-chip. *Annu. Rev. Fluid Mech.* **2004**, *36*, 381–411.

(28) Abécassis, B.; Cottin-Bizonne, C.; Ybert, C.; Ajdari, A.; Bocquet, L. Boosting migration of large particles by solute contrasts. *Nat. Mater.* **2008**, *7*, 785–789.

(29) Abécassis, B.; Cottin-Bizonne, C.; Ybert, C.; Ajdari, A.; Bocquet, L. Osmotic manipulation of particles for microfluidic applications. *New J. Phys.* **2009**, *11*, 075022.

(30) Shin, S. Diffusiophoretic separation of colloids in microfluidic flows. *Phys. Fluids* **2020**, *32*, 101302.

(31) Kar, A.; Chiang, T.-Y.; Ortiz-Rivera, I.; Sen, A.; Velegol, D. Enhanced transport into and out of dead-end pores. *ACS Nano* **2015**, *9*, 746–753.

(32) Shin, S.; Um, E.; Sabass, B.; Ault, J.; Rahimi, M.; Warren, P.; Stone, H. Size-dependent control of colloid transport via solute gradients in dead-end channels. *Proc. Natl. Acad. Sci. U.S.A.* **2016**, *113*, 257–261.

(33) Battat, S. Transport of Colloidal Particles by Diffusiophoresis. Senior Thesis, 2017, Princeton University.

(34) Battat, S.; Ault, J.; Shin, S.; Khodaparast, S.; Stone, H. Particle entrainment in dead-end pores by diffusiophoresis. *Soft Matter* **2019**, *15*, 3879–3885.

(35) Gupta, A.; Shim, S.; Stone, H. Diffusiophoresis: from dilute to concentrated electrolytes. *Soft Matter* **2020**, *16*, 6975–6984.

(36) Doan, V.; Saingam, P.; Yan, T.; Shin, S. A trace amount of surfactants enables diffusiophoretic swimming of bacteria. *ACS Nano* **2020**, *14*, 14219–14227.

(37) Wilson, J.; Shim, S.; Yu, Y.; Gupta, A.; Stone, H. Diffusiophoresis in multivalent electrolytes. *Langmuir* **2020**, *36*, 7014–7020.

(38) Alessio, B.; Shim, S.; Mintah, E.; Gupta, A.; Stone, H. Diffusiophoresis and diffusioosmosis in tandem: Two-dimensional particle motion in the presence of multiple electrolytes. *Phys. Rev. Fluids* **2021**, *6*, 054201.

(39) Banjeree, A.; Williams, I.; Nery-Azevedo, R.; Helgeson, M.; Squires, T. Soluto-inertial phenomena: Designing long-range, long-lasting, surface-specific interactions in suspensions. *Proc. Natl. Acad. Sci. U.S.A.* **2016**, *113*, 8612–8617.

(40) Shim, S.; Khodaparast, S.; Lai, C.-Y.; Yan, J.; J.T., A.; Rallabandi, B.; Shardt, O.; Stone, H. CO_2-driven diffusiophoresis for maintaining a bacteria-free surface. *Soft Matter* **2021**, *17*, 2568–2576.

(41) Florea, D.; Musa, S.; Huyghe, J.; Wyss, H. Long-range repulsion of colloids driven by ion exchange and diffusiophoresis. *Proc. Natl. Acad. Sci. U.S.A.* **2014**, *111*, 6554–6559.

(42) Musa, S.; Florea, D.; Wyss, H.; Huyghe, J. Convection associated with exclusion zone formation in colloidal suspensions. *Soft Matter* **2016**, *12*, 1127–1132.

(43) Cheng, Y.; Moraru, C. Long-range interactions keep bacterial cells from liquid-solid interfaces: Evidences of a bacteria exclusion zone near Nafion surfaces and possible implications for bacterial attachment. *Colloid Surface B* **2018**, *162*, 16–24.

(44) Paustian, J.; Nery-Azevedo, R.; Lundin, S.-T.; Gilkey, M.; Squires, T. Microfluidic microdialysis: Spatiotemporal control over solution microenvironments using integrated hydrogel membrane microwindows. *Phys. Rev. X* **2013**, *3*, 041010.

(45) Paustian, J.; Angulo, C.; Nery-Azevedo, R.; Shi, N.; Abdel-Fattah, A.; Squires, T. Direct measurements of colloidal solvophoresis under imposed solvent and solute gradients. *Langmuir* **2015**, *31*, 4402–4410.

(46) Shi, N.; Nery-Azevedo, R.; Abdel-Fattah, A.; Squires, T. Diffusiophoretic focusing of suspended colloids. *Phys. Rev. Lett.* **2016**, *117*, 258001.

(47) Nery-Azevedo, R.; Banerjee, A.; Squires, T. Diffusiophoresis in ionic surfactant gradients. *Langmuir* **2017**, *33*, 9694–9702.

(48) Shin, S.; Shardt, O.; Warren, P.; Stone, H. Membraneless water filtration using CO_2. *Nat. Commun.* **2017**, *8*.

(49) Shim, S.; Baskaran, M.; Thai, E.; Stone, H. CO_2-driven diffusiophoresis and water cleaning: Similarity solutions for predicting the exclusion zone in a channel flow. *Lab Chip* **2021**, *21*, 3387–3400.

(50) Lee, H.; Kim, J.; Yang, J.; Seo, S.; Kim, S. Diffusiophoretic exclusion of colloidal particles for continuous water purification. *Lab Chip* **2018**, *18*, 1713–1724.

(51) Lee, D.; Lee, J.; Lee, H.; Kim, S. Spontaneous selective preconcentration leveraged by ion exchange and imbibition through nanoporous medium. *Sci. Rep.* **2019**, *9*, 2336.

(52) Seo, M.; Park, S.; Lee, D.; Lee, H.; Kim, S. Continuous and spontaneous nanoparticle separation by diffusiophoresis. *Lab Chip* **2020**, *20*, 4118–4127.

(53) Lee, C.; Cottin-Bizonne, C.; Biance, A.-L.; Joseph, P.; Bocquet, L.; Ybert, C. Osmotic flow through fully permeable nanochannels. *Phys. Rev. Lett.* **2014**, *112*, 244501.

(54) Shin, S.; Ault, J.; Warren, P.; Stone, H. Accumulation of colloidal particles in flow junctions induced by fluid flow and diffusiophoresis. *Phys. Rev. X* **2017**, *7*, 041038.

(55) Ault, J.; Shin, S.; Stone, H. Diffusiophoresis in narrow channel flows. *J. Fluid Mech.* **2018**, *854*, 420–448.

(56) Rasmussen, M.; Pedersen, J.; Marie, R. Size and surface charge characterization of nanoparticles with a salt gradient. *Nat. Commun.* **2020**, *11*, 2337.

(57) Prieve, D.; Malone, S.; Khair, A.; Stout, R.; Kanj, M. Diffusiophoresis of charged colloidal particles in the limit of very high salinity. *Proc. Natl. Acad. Sci. U.S.A.* **2019**, *116*, 18257–18262.

(58) Williams, I.; Lee, S.; Apriceno, A.; Sear, R.; Battaglia, G. Diffusioosmotic and convective flows induced by a nonelectrolyte concentration gradient. *Proc. Natl. Acad. Sci. U.S.A.* **2020**, *117*, 25263–25271.

(59) Shim, S.; Stone, H. CO_2-leakage-driven diffusiophoresis causes spontaneous accumulation of charged materials in channel flow. *Proc. Natl. Acad. Sci. U.S.A.* **2020**, *117*, 25985—25990.

(60) Shimokusu, T.; Maybruck, V.; Ault, J.; S., S. Colloid separation by CO_2-induced diffusiophoresis. *Langmuir* **2020**, *36*, 7032–7038.

(61) Ha, D.; Seo, S.; Lee, K.; Kim, T. Dynamic transport control of colloidal particles by repeatable active switching of solute gradients. *ACS Nano* **2019**, *13*, 12939–12948.

(62) Palacci, J.; Abécassis, B.; Cottin-Bizonne, C.; Ybert, C.; Bocquet, L. Colloidal motility and pattern formation under rectified diffusiophoresis. *Phys. Rev. Lett.* **2010**, 138302.

(63) Palacci, J.; Cottin-Bizonne, C.; Ybert, C.; Bocquet, L. Osmotic traps for colloids and macromolecules based on logarithmic sensing in salt taxis. *Soft Matter* **2012**, *8*, 980–994.

(64) Wanunu, M.; Morrison, W.; Rabin, Y.; Grosberg, A.; Meller, A. Electrostatic focusing of unlabelled DNA into nanoscale pores using a salt gradient. *Nat. Nanotechnol.* **2010**, *5*, 160–165.

(65) Hatlo, M.; Panja, D.; van Roji, R. Translocation of DNA molecules through nanopores with salt gradients: The role of osmotic flow. *Phys. Rev. Lett.* **2011**, *107*, 068101.

(66) Li, S.; Li, A.; Hsieh, K.; Friedrich, S.; Wang, T.-H. Electrode-free concentration and recovery of DNA at physiologically relevant ionic concentrations. *Anal. Chem.* **2020**, *92*, 6150–6157.

(67) Friedrich, S.; Burke, J.; Liu, K.; Ivory, C.; Wang, T.-H. Molecular rheotaxis directs DNA migration and concentration against a pressure-driven flow. *Nat. Commun.* **2017**, *8*, 1213.

(68) Ramm, B.; Goychuk, A.; Khmelinskaia, A.; Blumhardt, P.; Eto, H.; Ganzinger, K.; Frey, E.; Schwille, P. A diffusiophoretic mechanism for ATP-driven transport without motor proteins. *Nat. Phys.* **2021**, *17*, 850–858.

(69) Vrhovec Hartman, S.; Božič, B.; Derganc, J. Migration of blood cells and phospholipid vesicles induced by concentration gradients in microcavities. *N. Biotechnol.* **2018**, *47*, 60–66.

(70) Hong, J.; Kim, B.; Shin, H. Mixed-scale poly(methyl methacrylate) channel network-based single-particle manipulation *via* diffusiophoresis. *Nanoscale* **2018**, *10*, 14421–14431.

(71) Moran, J.; Posner, J. Phoretic self-propulsion. *Annu. Rev. Fluid Mech.* **2017**, *49*, 11–40.

(72) Ohshima, H. Appropriate analytic expressions for the diffusiophoretic velocity of a spherical colloidal particle. *Electrophoresis* **2022**,

(73) Kirby, B.; Hasselbrink Jr., E. Zeta potential of microfluidic substrates: 1. Theory, experimental techniques, and effects on separations. *Electrophoresis* **2004**, *25*, 187–202.

(74) Kirby, B.; Hasselbrink Jr., E. Zeta potential of microfluidic substrates: 2. Data for polymers. *Electrophoresis* **2004**, *25*, 203–213.

(75) Gupta, A.; Rallabandi, B.; Stone, H. Diffusiophoretic and diffusioosmotic velocities for mixtures of valence-asymmetric electrolytes. *Phys. Rev. Fluids* **2019**, *4*, 043702.

(76) Chiang, T.-Y.; Velegol, D. Multi-ion diffusiophoresis. *J. Colloid Interface Sci.* **2014**, *424*, 120–123.

(77) Ohshima, H.; Furusawa, K. *Electrical Phenomena at Interfaces: Fundamentals, Measurements, and Applications*, 2nd ed.; Dekker: New York, 1998.

(78) Adamson, A.; Gast, A. *Physical Chemistry of Surfaces*, 6th ed.; John Wiley & Sons, 1997.

(79) Hunter, R. *Zeta Potential in Colloid Science: Principles and Applications*; Academic Press, 2013; Vol. 2.

(80) Healy, T. W.; White, L. R. Ionizable surface group models of aqueous interfaces. *Adv. Colloid Interface Sci.* **1978**, *9*, 303–345.

(81) Chu, H.; Garoff, S.; Tilton, R.; Khair, A. Advective-diffusive spreading of diffusiophoretic colloids under transient solute gradients. *Soft Matter* **2020**, *16*, 238–246.

(82) Persat, A.; Chambers, R.; Santiago, J. Basic principles of electrolyte chemistry for microfluidic electrokinetics. Part I: Acid-base equilibria and pH buffers. *Lab Chip* **2009**, *9*, 2437–2453.

(83) Persat, A.; Suss, M.; Santiago, J. Basic principles of electrolyte chemistry for microfluidic electrokinetics. Part II: Coupling between ion mobility, electrolysis, and acid-base equilibria. *Lab Chip* **2009**, *9*, 2454–2469.

(84) Shin, S.; Warren, P.; Stone, H. Cleaning by surfactant gradients: Particulate removal from porous materials and the significance of rinsing in laundry detergency. *Phys. Rev. Appl.* **2018**, *9*, 034012.

(85) Banerjee, A.; Tan, H.; Squires, T. Drop-in additives for suspension manipulation: Colloidal motion induced by sedimenting soluto-inertial beacons. *Phys. Rev. Fluids* **2020**, *5*, 073701.

(86) McDermott, J.; Kar, A.; Daher, M.; Klara, S.; Wang, G.; Sen, A.; Velegol, D. Self-generated diffusioosmotic flows from calcium carbonate micropumps. *Langmuir* **2012**, *28*, 15491–15497.

(87) Fukuyama, T.; Maeda, Y. Opto-thermal diffusiophoresis of soft biological matter: from physical principle to molecular manipulation. *Biophys. Rev.* **2020**, *12*, 309—-315.

(88) Guha, R.; Shang, X.; Zydney, A.; Velegol, D.; Kumar, M. Diffusiophoresis contributes significantly to colloidal fouling in low salinity reverse osmosis systems. *J. Membr. Sci.* **2015**, *479*, 67–76.

(89) Singh, N.; Vladisavljević, G.; Nadal, F.; Cottin-Bizonne, C.; Pirat, C.; Bolognesi, G. Reversible trapping of colloids in microgrooved channels via diffusiophoresis under steady-state solute gradients. *Phys. Rev. Lett.* **2020**, *125*, 248002.

(90) Gandhi, T.; Huang, J.; Aubret, A.; Li, Y.; Ramananarivo, S.; Vergassola, M.; Palacci, J. Decision-making at a T-junction by gradient-sensing microscopic agents. *Phys. Rev. Fluids* **2020**, *5*, 104202.

(91) Allen, R.; Saravis, C.; Maurer, H. *Gel Electrophoresis and Isoelectric Focusing of Proteins: Selected Techniques*; Walter de Gruyter: Berlin, New York, 1984.

(92) Janson, J. *Protein Purification: Principles, High Resolution Methods, and Applications*, 3rd ed.; John Wiley & Sons: Hoboken, New Jersey, 2011.

(93) Dorfman, K. DNA electrophoresis in microfabricated devices. *Rev. Mod. Phys.* **2010**, *82*, 2903–2947.

(94) Peter, Q.; Jacquat, R.; Herling, T.; Challa, P.; Kartanas, T.; Knowles, T. Microscale diffusiophoresis of proteins. October 2020, Preprint at Research Square. https://doi.org/10.21203/rs.3.rs-90645/v1 (accessed 2021-04-16).

(95) Lechlitner, L.; Annunziata, O. Macromolecule diffusiophoresis induced by concentration gradients of aqueous osmolytes. *Langmuir* **2018**, *34*, 9525–9531.

(96) McAfee, M.; Annunziata, O. Effect of particle size on salt-induced diffusiophoresis compared to Brownian mobility. *Langmuir* **2014**, *30*, 4916–4923.

(97) Fahim, A.; Annunziata, O. Amplification of salt-induced protein diffusiophoresis by varying salt from potassium to sodium to magnesium chloride in water. *Langmuir* **2020**, *36*, 2635–2643.

(98) Kodama, A.; Sakuma, Y.; Imai, M.; Kawakatsu, T.; Puff, N.; Angelova, M. Migration of phospholipid vesicles can be selectively driven by concentration gradients of metal chloride solutions. *Langmuir* **2017**, *33*, 10698–10706.

(99) Annunziata, O.; Buzatu, D.; Albright, J. Protein diffusiophoresis and salt osmotic diffusion in aqueous solutions. *J. Phys. Chem. B.* **2012**, *116*, 12694–12705.

(100) Sear, R. Diffusiophoresis in cells: A general nonequilibrium, nonmotor mechanism for the metabolism-dependent transport of particles in cells. *Phys. Rev. Lett.* **2019**, *122*, 128101.

(101) Qi, Y.; Adler, J. Salt taxis in *Escherichia coli* bacteria and its lack in mutants. *Proc. Natl. Acad. Sci. U.S.A.* **1989**, *86*, 8358–8362.

(102) Koshland, D. *Bacterial Chemotaxis as a Model Behavioral Systems*; Raven Press: New York, 1980.

(103) Wadhams, G.; Armitage, J. Making sense of it all: bacterial chemotaxis. *Nat. Rev. Mol. Cell Biol.* **2004**, *5*, 1024–1037.

(104) Ishizaki, T.; Hieda, J.; Bratescu, M.; Saito, N.; Takai, O. Biomimetic materials processing. Nanostructured Thin Films II. 2009; pp 104 – 115.

(105) Kosmulski, M.; Matijević, E. ζ-Potentials of Silica in Water-Alcohol Mixtures. *Langmuir* **1992**, *8*, 1060–1064.

(106) Li, R.; Wu, Z.; Wangb, Y.; Ding, L.; Wang, Y. Role of pH-induced structural change in protein aggregation in foam fractionation of bovine serum albumin. *Biotechnol. Rep.* **2016**, *9*, 46–52.

(107) Henry, N.; Clouet, J.; Le Visage, C.; Weiss, P.; Gautron, E.; Renard, D.; Cordonnier, T.; Boury, F.; Humbert, B.; Terrisse, H.; Guicheux, J.; Le Bideau, J. Silica nanofibers as a new drug delivery system: a study of the protein-silica interactions.

(108) Visan, A.; Lammertink, R. Reaction induced diffusio-phoresis of ordinary catalytic particles. *React. Chem. Eng.* **2019**, *4*, 1439–1446.

(109) Brown, A.; Poon, W. Ionic effects in self-propelled Pt-coated Janus swimmers. *Soft Matter* **2014**, *10*, 4016–4027.

(110) Yang, F.; Shin, S.; Stone, H. Diffusiophoresis of a charged drop. *J. Fluid Mech.* **2018**, *852*, 37–59.

(111) Shi, N.; Abdel-Fattah, A. Droplet migration into dead-end channels at high salinity enhanced by micelle gradients of a zwitterionic surfactant. *Phys. Rev. Fluids* **2021**, *6*, 053103.

(112) Banerjee, A.; Squires, T. Long-range, selective, on-demand suspension interactions: Combining and triggering soluto-inertial beacons. *Sci. Adv.* **2019**, eaax1893.

(113) Ahmed, T.; Shimizu, T.; Stocker, R. Microfluidic for bacterial chemotaxis. *Integr. Biol.* **2010**, *2*, 604–629.

(114) Ault, J.; Shin, S.; Stone, H. Characterization of surface-solute interactions by diffusioosmosis. *Soft Matter* **2019**, *15*, 1582–1596.

(115) Ahmed, T.; Stocker, R. Experimental verification of the behavioral foundation of bacterial transport parameters using microfluidics. *Biophys. J.* **2008**, *95*, 4481–4493.

(116) Tan, H.; Banerjee, A.; Shi, N.; Tang, X.; Abdel-Fattah, A.; Squires, T. A two-step strategy for delivering particles to targets hidden within microfabricated porous media. *Sci. Adv.* **2021**, *7*, eabh0638.

(117) Yang, D.; Jennings, A.; Borrego, E.; Retterer, S.; Männik, J. Analysis of factors limiting bacterial growth in PDMS mother machine devices. *Frontiers in Microbiology* **2018**, *9*.

(118) Gupta, A.; Shim, S.; Issah, L.; C., M.; Stone, H. Diffusion of multiple electrolytes cannot be treated independently: model predictions with experimental validation. *Soft Matter* **2019**, *15*, 9965–9973.

(119) Ault, J.; Warren, P.; Shin, S.; Stone, H. Diffusiophoresis in one-dimensional solute gradients. *Soft Matter* **2017**, *13*, 9015–9023.

(120) Hoshyargar, V.; Ashrafizadeh, S.; Sadeghi, A. Diffusioosmotic flow in rectangular microchannels. *Electrophoresis* **2016**, *37*, 809–817.

(121) Pan, F.; Acrivos, A. Steady flows in rectangular cavities. *J. Fluid Mech.* **1967**, *28*, 643–655.

(122) Tanase, N.-O.; Simionescu, S.-M.; Broboana, D.; Balan, C. Experimental and numerical studies of the cavity flows at low Reynolds numbers. *Energy Procedia* **2017**, *112*, 210–216.

(123) Iwatsu, R.; Ishii, K.; Kawamuru, T.; Kuwahara, K.; Hyun, J. Numerical simulation of three-dimensional flow structure in a driven cavity. *Fluid Dyn. Res.* **1989**, *5*, 173–189.

(124) Bretherton, F. The motion of long bubbles in tubes. *J. Fluid Mech.* **1961**, *10*, 166–188.

(125) Khodaparast, S.; Atasi, O.; Scheid, B.; Stone, H. Dewetting of thin liquid films surrounding air bubble in microchannels. *Langmuir* **2017**, *34*, 1363–1370.

(126) Magnini, M.; Municchi, F.; El Mellas, I.; Icardi, M. Liquid film distribution around long gas bubbles propagating in rectangular capillaries. *Int. J. Multiph. Flow* **2022**, *148*, 103939.

(127) Baroud, C.; Gallaire, F.; Dangla, R. Dynamics of microfluidic droplets. *Lab Chip* **2010**, *10*, 2032–2045.

(128) Roman, S.; Soulaine, C.; Kovscek, A. Pore-scale visualization and characterization of viscous dissipation in porous media. *J. Colloid Interface Sci.* **2020**, *558*, 269–279.

(129) Shim, S.; Wan, J.; Hilgenfeldt, S.; Panchal, P.; Stone, H. Dissolution without disappearing: multicomponent gas exchange for CO_2 bubbles in a microfluidic channel. *Lab Chip* **2014**, *14*, 2428–2436.

(130) Giddings, J.; Yang, F.; Myers, M. Flow field-flow fractionation: A versatile new separation method. *Science* **1976**, *193*, 1244–1245.

(131) Giddings, J. Field-flow fractionation: Analysis of macromolecular, colloidal, and particulate materials. *Science* **1993**, *260*, 1456–1465.

(132) Shendruk, T.; Tahvildari, R.; Catafard, N.; Andrzejewski, L.; Gigault, C.; Todd, A.; Gagne-Dumais, L.; Slater, G.; Godin, M. Field-flow fractionation and hydrodynamic chromatography on a microfluidic chip. *Anal. Chem.* **2013**, *85*, 5981–5988.

(133) Deen, W. M. *Analysis of Transport Phenomena*; Oxford University Press, 2012.

(134) Leal, L. *Advanced Transport Phenomena*; Cambridge University Press, 2007.

(135) Lee, D.; Kim, S. Spontaneous diffusiophoretic separation in paper-based microfluidic device. *Micro and Nano Syst. Lett.* **2020**, *8*, 6.

(136) Salek, M.; Carrara, F.; Fernandez, V.; Guasto, J.; Stocker, R. Bacterial chemotaxis in a microfluidic T-maze reveals strong phenotypic heterogeneity in chemotactic sensitivity. *Nat. Commun.* **2019**, *10*, 1877.

(137) Lee, J.; Lee, K.; Wang, C.; Ha, D.; Kim, G.-H.; Park, J.; Kim, T. Combined Effects of Zeta-potential and Temperature of Nanopores on Diffusioosmotic Ion Transport. *Anal. Chem.* **2021**, *93*, 14169–14177.

(138) Hillen, T.; Painter, K. A user's guide to PDE models for chemotaxis. *J. Math. Biol.* **2009**, *58*, 183–217.

(139) Möller, F.; Kriegel, F.; Kieß, M.; Sojo, V.; Braun, D. Steep pH gradients and directed colloid transport in a microfluidic alkaline hydrothermal pore. *Angew. Chem. Int. Ed.* **2017**, *56*, 2340–2344.

(140) de Anna, P.; Pahlavan, A. A.; Yawata, Y.; Stocker, R.; Juanes, R. Chemotaxis under flow disorder shapes microbial dispersion in porous media. *Nat. Phys.* **2021**, *17*, 68–73.

(141) Aminian, M.; Bernardi, F.; Camassa, R.; Harris, D.; McLaughlin, R. How boundaries shape chemical delivery in microfluidics. *Science* **2016**, *354*, 1252–1256.

(142) Chiu, H.; Keh, H. Diffusiophoresis of a charged particle in a microtube. *Electrophoresis* **2017**, *38*, 2468–2478.

(143) Tseng, S.; Chung, Y.-C.; Hsu, J.-P. Diffusiophoresis of a soft, pH-regulated particle in a solution containing multiple ionic species. *J. Colloid Interface Sci.* **2015**, *438*, 196–203.

(144) Ohshima, H. Diffusiophoretic velocity of a spherical soft particle. *Colloid Polym. Sci.* **2022**,

(145) Das, S.; Shklyaev, O.; Altemose, A.; Shum, H.; Ortiz-Rivera, I.; Valdez, L.; Mallouk, T.; Balazs, A.; Sen, A. Harnessing catalytic pumps for directional delivery of microparticles in microchambers. *Nat. Commun.* **2017**, *8*, 14384.

TOC Graphic

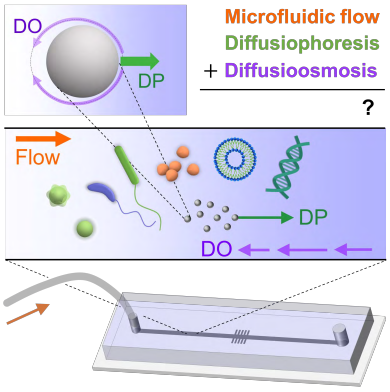
DO
DP
Microfluidic flow
Diffusiophoresis
+ Diffusioosmosis
?
Flow
DP
DO